

Constituent quarks and g_1

Steven D. Bass *

*Max Planck Institut für Kernphysik, Postfach 103 980,
D-69029 Heidelberg, Germany*

*Institut für Theoretische Physik,
Physik Department, Technische Universität München,
D-85747 Garching, Germany*

Abstract

We review the theory and present status of the proton spin problem with emphasis on the transition between current quarks and constituent quarks in QCD.

*Steven.Bass@physik.tu-muenchen.de

1 Introduction

Polarised deep inelastic scattering experiments at CERN [1, 2, 3, 4], DESY [5] and SLAC [6, 7, 8, 9] have revealed an apparent two (or more) standard deviations violation of OZI in the flavour-singlet axial charge $g_A^{(0)}$ which is extracted from the first moment of g_1 (the nucleon's first spin dependent structure function). This discovery has inspired much theoretical and experimental effort to understand the internal spin structure of the nucleon.

In this article we review the theory and present status of the proton spin problem in QCD. We start with a simple sum-rule for the spin of the proton ($+\frac{1}{2}$) in terms of the angular momentum of its quark and gluonic constituents:

$$\frac{1}{2} = \frac{1}{2}\Sigma + L_z + \Delta g. \quad (1)$$

Here, $\frac{1}{2}\Sigma$ and Δg are the quark and gluonic intrinsic spin contributions to the nucleon's spin and L_z is the orbital contribution. One would like to understand the spin decomposition, Eq.(1), both in terms of the fundamental QCD quarks and gluons and also in terms of the constituent quark quasi-particles of low-energy QCD.

In deep inelastic processes the internal structure of the nucleon is described by the QCD parton model [10]. The deep inelastic structure functions may be written as the sum over the convolution of “soft” quark and gluon parton distributions with “hard” photon-parton scattering coefficients. The (target dependent) parton distributions describe a flux of quark and gluon partons carrying some fraction $x = p_{\text{parton}}/p_{\text{proton}}$ of the proton's momentum into the hard (target independent) photon-parton interaction which is described by the hard scattering coefficients.

In low energy processes the nucleon behaves like a colour neutral system of three massive constituent quark quasi-particles interacting self consistently with a cloud of virtual pions which is induced by spontaneous chiral symmetry breaking [11, 12, 13].

One of the most challenging problems in particle physics is to understand the transition between the fundamental QCD “current” quarks and gluons and the constituent quarks of low-energy QCD. The fundamental building blocks are the local QCD quark and gluon fields together with the non-local structure [14] associated with gluon topology [15].

The large mass of the constituent quarks is usually understood in terms of dynamical chiral symmetry breaking and the interaction of the current quarks with a scalar condensate (in the Nambu-Jona-Lasinio model [16, 12, 13]) or in terms of scalar confinement (in the Bag model [11]).

Through the axial anomaly in QCD [17, 18, 15], some fraction of the spin of the nucleon and of the constituent quark is carried by its quark and gluon partons and some fraction is carried by gluon topology [19]. The topological winding number is a global property of the theory; it is independent of the local quark and gluon

fields. When we take the Fourier transform to momentum space any topological contribution to the nucleon's spin has support only at $x = 0$. This means that whereas the nucleon's momentum is given by the sum of the momenta of the partons

$$\sum_{\text{partons}} x_i = 1 \quad (2)$$

one has to be careful about writing equations such as

$$\frac{1}{2} \stackrel{?}{=} \left(\frac{1}{2} \Sigma + L_z + \Delta g \right)_{\text{partons}}. \quad (3)$$

Some fraction of the nucleon's spin may reside at Bjorken $x = 0$. This effect may be viewed as a deformation of the QCD θ vacuum [14] inside a nucleon due to tunneling processes between vacuum states with different topological winding number.

In semi-classical quark models the quark spin content Σ is equal to the nucleon's flavour singlet axial charge $g_A^{(0)}$. Relativistic quark-pion coupling models predict $g_A^{(0)} \simeq 0.6$ with about 40% of the proton's spin being carried by orbital angular momentum [20, 21].

The value of $g_A^{(0)}$ which is extracted from polarised deep inelastic scattering experiments is $g_A^{(0)}|_{\text{pDIS}} \simeq 0.2 - 0.35$ [1-9]; — significantly less than the semi-classical prediction for $g_A^{(0)}$.

In QCD the axial anomaly induces various gluonic contributions to the flavour singlet axial charge $g_A^{(0)}$. Explanations of the small value of $g_A^{(0)}|_{\text{pDIS}}$ have been proposed based on the QCD parton model [22, 23, 24] and non-perturbative chiral $U_A(1)$ dynamics [25-31]. One finds [22, 23, 24, 19]

$$g_A^{(0)} = \left(\sum_q \Delta q - f \frac{\alpha_s}{2\pi} \Delta g \right)_{\text{partons}} + \mathcal{C} \quad (4)$$

where f ($=3$) is the number of light flavours liberated into the final state. Here $\frac{1}{2}\Delta q$ and Δg are the amount of spin carried by quark and gluon partons in the polarised proton and \mathcal{C} measures the gluon-topological contribution to $g_A^{(0)}$ [19].

The topological term \mathcal{C} has support only at $x = 0$; it is missed by polarised deep inelastic scattering experiments which measure the combination $g_A^{(0)}|_{\text{pDIS}} = (g_A^{(0)} - \mathcal{C})$. If some fraction of the spin of the constituent quark is carried by gluon topology in QCD, then the constituent quark model predictions for $g_A^{(0)}$ are not necessarily in contradiction with the small value of $(g_A^{(0)} - \mathcal{C})$ extracted from deep inelastic scattering experiments. In Section 5 we explain a simple dynamical mechanism for producing such an effect.

If there is no topological $x = 0$ term, then the small value of $g_A^{(0)}|_{\text{pDIS}}$ would be consistent with the semi-classical prediction for Σ if Δg is both large and positive ($\sim +1.5$ at $Q^2 \simeq 1\text{GeV}^2$). If discovered in future experiments, such a large Δg

would pose a challenge for constituent quark models which do not naturally include such an effect.

In this article we review our present understanding of the spin structure of the nucleon, both at the constituent quark level and in QCD. We emphasise present and future experiments which could help to unravel the nucleon's internal spin structure by separately measuring the Δq_{parton} , Δg_{parton} and \mathcal{C} contributions to $g_A^{(0)}$. The structure of the paper is as follows. In Section 2 we give a brief introduction to deep inelastic scattering and the polarised deep inelastic measurements of the nucleon's axial charges $g_A^{(k)}$. In Section 3 we review the theoretical interpretation of the axial charges $g_A^{(k)}$ and the OZI violation observed in deep inelastic measurements of $g_A^{(0)}$. The connection between chiral symmetry and the spin structure of the nucleon is emphasised in Section 3.4. Sections 4-6 are more technical. In Section 4 we review the axial anomaly in QCD and its role in our understanding of the physics of $g_A^{(0)}$. In Section 5 we discuss the relationship between gluon topology and the spin structure of the nucleon. Section 6 gives an overview of the QCD parton model and its application to polarised deep inelastic scattering. In Section 7 we discuss the shape of g_1 and the x dependence of the various contributions to the nucleon's axial charges and $\int_0^1 dx g_1(x, Q^2)$. Finally, in Section 8, we summarise the information about the spin structure of the nucleon which can be learnt in present and future experiments.

We refer to Refs.[32-38] for further reviews on the spin structure of the nucleon in polarised deep inelastic scattering and to Ref.[39] for a review of polarised photoproduction and the transition to polarised deep inelastic scattering.

2 The spin structure function g_1

2.1 Polarised deep inelastic scattering

Our present knowledge about the spin structure of the nucleon comes from polarised deep inelastic scattering experiments. These experiments involve scattering a high-energy charged lepton beam from a nucleon target at large momentum transfer squared. One measures the inclusive cross-section. The lepton beam (electrons at DESY and SLAC and muons at CERN) is longitudinally polarised. The nucleon target may be either longitudinally or transversely polarised.

Consider polarised $e - p$ scattering.

We work in one photon exchange approximation. Whilst the electron photon vertex is described by perturbative QED, the internal QCD structure of the proton means that the photon proton interaction is described in terms of various structure functions (form-factors).

Let p_μ , m and s_μ denote the momentum, mass and spin of the target proton and q_μ denote the momentum of the exchanged photon. Define $Q^2 = -q^2$ and $\nu = p \cdot q$.

Deep inelastic scattering involves working in the Bjorken limit: Q^2 and ν both $\rightarrow \infty$ with the Bjorken variable $x = \frac{Q^2}{2p \cdot q}$ held fixed.

We specialise to the target rest frame and let E denote the energy of the incident electron which is scattered through an angle θ to emerge in the final state with energy E' . Let $\uparrow\downarrow$ denote the longitudinal polarisation of the beam and $\uparrow\downarrow$ denote a longitudinally polarised proton target. The unpolarised and polarised differential cross-sections are:

$$\left(\frac{d^2\sigma}{d\Omega dE'} \uparrow\uparrow + \frac{d^2\sigma}{d\Omega dE'} \uparrow\downarrow \right) = \frac{8\alpha^2(E')^2}{mQ^4} \left[2 \sin^2 \frac{\theta}{2} F_1(x, Q^2) + \frac{m^2}{\nu} \cos^2 \frac{\theta}{2} F_2(x, Q^2) \right] \quad (5)$$

and

$$\left(\frac{d^2\sigma}{d\Omega dE'} \uparrow\uparrow - \frac{d^2\sigma}{d\Omega dE'} \uparrow\downarrow \right) = \frac{4\alpha^2 E'}{Q^2 E \nu} \left[(E + E' \cos \theta) g_1(x, Q^2) - 2xm g_2(x, Q^2) \right]. \quad (6)$$

Here F_1 and F_2 denote the nucleon's first and second spin independent structure functions; g_1 and g_2 denote the first and second spin dependent structure functions. The structure functions contain all of the target dependent information in the deep inelastic process.

The unpolarised structure functions have been measured in experiments at CERN, DESY, FNAL and SLAC. We refer to [40, 41] for recent reviews of these data and the interpretation of F_1 and F_2 .

Polarised deep inelastic scattering experiments with longitudinally polarised targets provide the cleanest probe of g_1 . In a fixed target experiment the contribution of the second spin structure function g_2 to the differential cross section, Eq.(6), is suppressed relative to the g_1 contribution by the kinematic factor $\frac{m}{E}$. In deep inelastic experiments $\frac{m}{E}$ is typically less than 0.03 and the g_2 contribution to Eq.(6) becomes lost among the experimental errors. The structure function g_2 can be measured using a transversely polarised target. In this case the two spin structure functions g_1 and g_2 contribute to the spin dependent part of the total cross section with equal weight:

$$\left(\frac{d^2\sigma}{d\Omega dE'} \uparrow\Rightarrow - \frac{d^2\sigma}{d\Omega dE'} \uparrow\Leftarrow \right) = \frac{4\alpha^2 E'^2}{Q^2 E \nu} \sin \theta \left[g_1(x, Q^2) + \frac{2Em}{\nu} g_2(x, Q^2) \right]. \quad (7)$$

The experimental programme in polarised deep inelastic scattering has so far mainly focussed on measurements of g_1 . The first measurements of g_2 have recently been reported by the SMC and SLAC E-143 and E-154 collaborations [42]. In this review we focus on the physics of g_1 . We refer to Jaffe [43] for a theoretical review of g_2 .

2.2 The first moment of g_1

When $Q^2 \rightarrow \infty$, the light-cone operator product expansion relates the first moment of the structure function g_1 to the scale-invariant axial charges of the target nucleon by [44, 45, 46, 47]

$$\begin{aligned} \int_0^1 dx g_1^p(x, Q^2) &= \left(\frac{1}{12} g_A^{(3)} + \frac{1}{36} g_A^{(8)} \right) \left\{ 1 + \sum_{\ell \geq 1} c_{\text{NS}\ell} \alpha_s^\ell(Q) \right\} \\ &+ \frac{1}{9} g_A^{(0)}|_{\text{inv}} \left\{ 1 + \sum_{\ell \geq 1} c_{\text{S}\ell} \alpha_s^\ell(Q) \right\} + \mathcal{O}\left(\frac{1}{Q^2}\right). \end{aligned} \quad (8)$$

Here $g_A^{(3)}$, $g_A^{(8)}$ and $g_A^{(0)}|_{\text{inv}}$ are the isotriplet, SU(3) octet and scale-invariant flavour-singlet axial charges respectively. The flavour non-singlet $c_{\text{NS}\ell}$ and singlet $c_{\text{S}\ell}$ coefficients are calculable in ℓ -loop perturbation theory and have been calculated to $\mathcal{O}(\alpha_s^3)$ precision [47].

The first moment of g_1 is constrained by low energy weak interactions. For proton states $|p, s\rangle$ with momentum p_μ and spin s_μ

$$\begin{aligned} 2ms_\mu g_A^{(3)} &= \langle p, s | (\bar{u}\gamma_\mu\gamma_5 u - \bar{d}\gamma_\mu\gamma_5 d) | p, s \rangle_c \\ 2ms_\mu g_A^{(8)} &= \langle p, s | (\bar{u}\gamma_\mu\gamma_5 u + \bar{d}\gamma_\mu\gamma_5 d - 2\bar{s}\gamma_\mu\gamma_5 s) | p, s \rangle_c \end{aligned} \quad (9)$$

where the subscript c denotes the connected matrix element. The isotriplet axial charge $g_A^{(3)}$ is measured independently in neutron beta decays: $g_A^{(3)} = 1.267 \pm 0.004$ [48]. Modulo SU_F(3) breaking [49], the flavour octet axial charge $g_A^{(8)}$ is measured independently in hyperon beta decays: $g_A^{(8)} = 0.58 \pm 0.03$. The scale-invariant flavour-singlet axial charge $g_A^{(0)}|_{\text{inv}}$ is defined by [50]

$$2ms_\mu g_A^{(0)}|_{\text{inv}} = \langle p, s | E(\alpha_s) J_{\mu 5}^{GI} | p, s \rangle_c \quad (10)$$

where

$$J_{\mu 5}^{GI} = (\bar{u}\gamma_\mu\gamma_5 u + \bar{d}\gamma_\mu\gamma_5 d + \bar{s}\gamma_\mu\gamma_5 s)_{GI} \quad (11)$$

is the gauge-invariantly renormalised singlet axial-vector operator and

$$E(\alpha_s) = \exp \int_0^{\alpha_s} d\tilde{\alpha}_s \gamma(\tilde{\alpha}_s) / \beta(\tilde{\alpha}_s) \quad (12)$$

is a renormalisation group factor which corrects for the (two loop) non-zero anomalous dimension $\gamma(\alpha_s)$ ($= f \frac{\alpha_s^2}{\pi^2} + \mathcal{O}(\alpha_s^3)$) of $J_{\mu 5}^{GI}$ [51, 15, 46]. In Eq.(12) $\beta(\alpha_s)$ is the QCD beta function. We are free to choose the QCD coupling $\alpha_s(\mu)$ at either a hard or a soft scale μ . The singlet axial charge $g_A^{(0)}|_{\text{inv}}$ is independent of the renormalisation scale μ . It may be measured independently in an elastic neutrino proton scattering experiment [52].

Polarised deep inelastic scattering experiments measure $g_1(x, Q^2)$ between some small but finite value x_{min} and an upper value x_{max} which is close to one. Deep

inelastic measurements of $g_A^{(3)}$ and $g_A^{(0)}|_{\text{inv}}$ involve a smooth extrapolation of the g_1 data to $x = 0$ which is motivated either by Regge theory or by perturbative QCD. As we decrease $x_{\min} \rightarrow 0$ we measure the first moment

$$\Gamma \equiv \lim_{x_{\min} \rightarrow 0} \int_{x_{\min}}^1 dx g_1(x, Q^2). \quad (13)$$

Polarised deep inelastic experiments cannot, even in principle, measure at $x = 0$ with finite Q^2 . They miss any possible $\delta(x)$ terms which might exist in g_1 at large Q^2 .

Assuming no isotriplet $\delta(x)$ term in g_1 , polarised deep inelastic scattering experiments at CERN [1, 2, 3, 4], DESY [5] and SLAC [8, 9] have verified the Bjorken sum-rule [44]

$$I_{Bj} = \int_0^1 dx (g_1^p - g_1^n) = \frac{g_A^{(3)}}{3} \left[1 - \frac{\alpha_s}{\pi} - 3.58 \left(\frac{\alpha_s}{\pi} \right)^2 - 20.21 \left(\frac{\alpha_s}{\pi} \right)^3 \right] \quad (14)$$

for the isovector part of g_1 to 10% accuracy. They have also revealed an apparent two standard deviations violation of OZI in the flavour singlet axial charge extracted from polarised deep inelastic scattering:

$$g_A^{(0)}|_{\text{pDIS}} = 0.2 - 0.35. \quad (15)$$

This number compares with $g_A^{(8)} = 0.58 \pm 0.03$ from hyperon beta-decays [49].

The small x extrapolation of g_1 data is presently the largest source of experimental error on measurements of the nucleon's axial charges from deep inelastic scattering.

3 Interpretation of $g_A^{(k)}$

The small value of $g_A^{(0)}|_{\text{pDIS}}$ measured in polarised deep inelastic scattering has inspired many theoretical ideas about the spin structure of the nucleon. The original EMC measurement [1] of $g_A^{(0)}|_{\text{pDIS}}$ came as a surprise since, in the pre-QCD parton model, $g_A^{(0)}$ is interpreted as the fraction of the proton's spin which is carried by the spin of its quarks — and since the original EMC measurement was consistent with zero! It is amusing to speculate how QCD might have developed if that measurement had been available and current at the time when Gell-Mann and collaborators discovered the Eightfold Way symmetry.

How should we interpret the axial charges $g_A^{(k)}$ in QCD ?

Define

$$2ms_\mu \Delta q = \langle p, s | \left(\bar{q} \gamma_\mu \gamma_5 q \right)_{GI} | p, s \rangle_c. \quad (16)$$

The axial charges may be written

$$\begin{aligned}
g_A^{(3)} &= \Delta u - \Delta d \\
g_A^{(8)} &= \Delta u + \Delta d - 2\Delta s \\
g_A^{(0)} \equiv g_A^{(0)}|_{\text{inv}}/E(\alpha_s) &= \Delta u + \Delta d + \Delta s.
\end{aligned} \tag{17}$$

The non-singlet axial charges are scale invariant. The flavour-singlet combination $g_A^{(0)} = \Delta u + \Delta d + \Delta s$ depends on the renormalisation scale μ ; it evolves with the two loop anomalous dimension $\gamma(\alpha_s)$. The scale dependent $g_A^{(0)}(\mu^2)$ is frequently used in theoretical descriptions of deep inelastic scattering where it is common to set the renormalisation scale μ^2 equal to the virtuality Q^2 of the hard photon, make a perturbative expansion of $E(\alpha_s)$ and then absorb $E(\alpha_s)$ into the singlet Wilson coefficient $\{1 + \sum_{\ell \geq 1} c_{\text{S}\ell} \alpha_s^\ell(Q)\}$. While this is a legitimate theoretical procedure for describing the first moment of g_1 at large Q^2 it is important to bear in mind that physical observables do not depend on the theorist's choice of renormalisation scale. $g_A^{(0)}|_{\text{inv}}$ is a physical observable whereas the renormalisation-scale dependent $g_A^{(0)}(\mu^2)$ is not [53].

In the rest of this Section we discuss the interpretation of the axial charges $g_A^{(k)}$ in constituent quark models (Section 3.1) and in QCD (Sections 3.2 and 3.3). In Section 3.4 we highlight the relation between chiral symmetry and the spin structure of the nucleon.

3.1 Constituent quarks and $g_A^{(k)}$

In semi-classical quark models Δq is interpreted as the amount of spin carried by quarks and antiquarks of flavour q , there is no $E(\alpha_s)$ factor and $\Sigma = g_A^{(0)}$. Relativistic quark-pion coupling models such as the Cloudy Bag [11] which contain no explicit strange quark or gluon degrees of freedom ¹ predict $g_A^{(0)} = g_A^{(8)}$. Whilst these models do not explain the small value of $g_A^{(0)}|_{\text{pDIS}}$ they do give a good account of the flavour non-singlet axial charges $g_A^{(3)}$ and $g_A^{(8)}$.

First, consider the static quark model. The simple SU(6) proton wavefunction

$$\begin{aligned}
|p \uparrow\rangle &= \frac{1}{\sqrt{2}}|u \uparrow (ud)_{S=0}\rangle + \frac{1}{\sqrt{18}}|u \uparrow (ud)_{S=1}\rangle - \frac{1}{3}|u \downarrow (ud)_{S=1}\rangle \\
&\quad - \frac{1}{3}|d \uparrow (uu)_{S=1}\rangle + \frac{\sqrt{2}}{3}|d \downarrow (uu)_{S=1}\rangle
\end{aligned} \tag{18}$$

yields $g_A^{(3)} = \frac{5}{3}$ and $g_A^{(8)} = g_A^{(0)} = 1$.

In relativistic quark models one has to take into account the four-component Dirac spinor $\psi = \begin{pmatrix} f \\ \sigma \cdot \hat{r} g \end{pmatrix}$. The lower component of the Dirac spinor is p-wave with intrinsic spin primarily pointing in the opposite direction to spin of the nucleon.

¹The gluonic degrees of freedom are integrated out into the confinement potential.

Relativistic effects renormalise the NRQM axial charges by a factor $(f^2 - \frac{1}{3}g^2)$ with a net transfer of angular momentum from intrinsic spin to orbital angular momentum. In the MIT Bag $(f^2 - \frac{1}{3}g^2) = 0.65$ reducing $g_A^{(3)}$ from $\frac{5}{3}$ to 1.09. Centre of mass motion then increases the axial charges by about 20% bringing $g_A^{(3)}$ close to its physical value 1.27².

The pion cloud of the nucleon also renormalises the nucleon's axial charges by shifting intrinsic spin into orbital angular momentum. Consider the Cloudy Bag Model (CBM). Here, the Fock expansion of the nucleon in terms of a bare MIT nucleon $|N\rangle$ and baryon-pion $|N\pi\rangle$ $|\Delta\pi\rangle$ Fock states converges rapidly. We may safely truncate the Fock expansion at the one pion level. The CBM axial charges are [20]:

$$\begin{aligned} g_A^{(3)} &= \frac{5}{3}\mathcal{N}\left(1 - \frac{8}{9}P_{N\pi} - \frac{4}{9}P_{\Delta\pi} + \frac{8}{15}P_{N\Delta\pi}\right) \\ g_A^{(0)} &= \mathcal{N}\left(1 - \frac{4}{3}P_{N\pi} + \frac{2}{3}P_{\Delta\pi}\right). \end{aligned} \quad (19)$$

Here, \mathcal{N} takes into account the relativistic factor $(f^2 - \frac{1}{3}g^2)$ and centre of mass motion in the Bag. The coefficients $P_{N\pi} = 0.2$ and $P_{\Delta\pi} = 0.1$ denote the probabilities to find the physical nucleon in the $|N\pi\rangle$ and $|\Delta\pi\rangle$ Fock states respectively and $P_{N\Delta\pi} = 0.3$ is the interference term. The bracketed pion cloud renormalisation factors in Eq.(19) are 0.94 for $g_A^{(3)}$ and 0.8 for $g_A^{(0)}$. Through the Goldberger-Treiman, the small pion cloud renormalisation of $g_A^{(3)}$ translates into a small pion cloud renormalisation of $g_{\pi NN}$, which is necessary to treat the pion cloud in low order perturbation theory [11]. With a 20% centre of mass correction, the CBM predicts $g_A^{(3)} \simeq 1.25$ and $g_A^{(0)} = g_A^{(8)} \simeq 0.6$. Similar numbers [21] are obtained in the Nambu-Jona-Lasinio model.

Including kaon loops into the model generates a small $\Delta s \simeq -0.003$ [55] in the Cloudy Bag Model and -0.006 [21] in the Nambu-Jona-Lasinio model. These values are an order of magnitude smaller than the value of Δs extracted from polarised deep inelastic scattering experiments by combining Eq.(15) with $g_A^{(8)}$: Δs between -0.13 and -0.07.

In QCD the axial anomaly induces various gluonic contributions to $g_A^{(0)}$. Since gluons are flavour singlet, it follows that, modulo flavour SU(3) breaking, explicit gluonic contributions to Δq will cancel in the isotriplet and SU(3) octet axial charges $g_A^{(3)}$ and $g_A^{(8)}$.

3.2 The renormalisation group factor $E(\alpha_s)$

The first QCD effect that we consider is the renormalisation group factor $E(\alpha_s)$. The scale dependent axial charge $g_A^{(0)}$ is related to the scale invariant $g_A^{(0)}|_{\text{inv}}$ by

² The renormalisation of $g_A^{(3)}$ from $\frac{5}{3}$ to $\simeq 1.25$ is also found in light-cone binding models [54].

$$g_A^{(0)} = g_A^{(0)}|_{\text{inv}}/E(\alpha_s).$$

One popular idea [56, 57] is that the physics of confinement and dynamical symmetry breaking determines the parton distributions at some low scale $\mu_0^2 \sim 0.3\text{GeV}^2$. Parton distributions may be calculated at the scale μ_0^2 using one's favourite quark model, evolved using perturbative QCD to deep inelastic values of Q^2 and then compared with data. In this approach it is natural to associate the quark model predictions of $g_A^{(0)}$ with $g_A^{(0)}(\mu_0^2)$ instead of the scale-invariant quantity $g_A^{(0)}|_{\text{inv}}$ in QCD.

How big is $E(\alpha_s)$?

The perturbative QCD expansion of $E(\alpha_s)$ is

$$\begin{aligned} E(\alpha_s) &= 1 - \frac{24f}{33-2f} \frac{\alpha_s}{4\pi} \\ &+ \frac{1}{2} \left(\frac{\alpha_s}{4\pi} \right)^2 \frac{f}{33-2f} \left(\frac{16f}{3} - 472 + 72 \frac{102 - \frac{14f}{3}}{33-2f} \right) + \mathcal{O}(\alpha_s^3) \end{aligned} \quad (20)$$

where f is the number of flavours. To $\mathcal{O}(\alpha_s^2)$ the perturbative expansion (20) remains close to one – even for large values of α_s . If we take $\alpha_s \sim 0.6$ as typical of the infra-red ³ then

$$E(\alpha_s) \simeq 1 - 0.13 - 0.03 = 0.84. \quad (21)$$

Here -0.13 and -0.03 are the $\mathcal{O}(\alpha_s)$ and $\mathcal{O}(\alpha_s^2)$ corrections respectively. Perturbative QCD evolution is insufficient to reduce the flavour-singlet axial-charge from its naive value 0.6 to the value (15) extracted from polarised deep inelastic scattering.

3.3 Gluons and $g_A^{(0)}$

In QCD the axial anomaly [17, 18] induces various gluonic contributions to $g_A^{(0)}$. One finds [22, 23, 24, 19]

$$g_A^{(0)} = \left(\sum_q \Delta q - f \frac{\alpha_s}{2\pi} \Delta g \right)_{\text{partons}} + \mathcal{C} \quad (22)$$

where f ($=3$) is the number of light-quark flavours. Here Δq_{parton} and Δg_{parton} are interpreted as the amount of spin carried by quark and gluon partons in the polarised nucleon and \mathcal{C} measures any contribution to $g_A^{(0)}$ from gluon topology [19]. In leading order QCD evolution Δg_{parton} evolves as $1/\alpha_s$ so the product $-\frac{\alpha_s}{2\pi} \Delta g_{\text{parton}}$ scales at very large Q^2 [23].

The three terms in Eq.(22) are separately measurable. We now outline the physics associated with each of these three contributions — a detailed discussion is given in Sections 4-6 below.

³ The coupling $\alpha_s(\mu_0^2) \simeq 0.6$ is the optimal model input which is found in both the GRV [56] and Bag Model [58] fits to deep inelastic structure function data. It is interesting to note that this is the same coupling where Gribov [59] suggested that perturbative QCD should give way to something approaching a constituent-quark pion coupling model.

The QCD parton model [10] describes g_1 at finite x (greater than zero). The polarised gluon contribution to Eq.(22) is characterised by the contribution to the first moment of g_1 from two-quark-jet events carrying large transverse momentum squared $k_T^2 \sim Q^2$ [24] which are generated by photon-gluon fusion — see Section 6. The polarised quark contribution Δg_{parton} is associated with the first moment of the measured g_1 after these two-quark-jet events are subtracted from the total data set.

The term \mathcal{C} measures any topological contribution to $g_A^{(0)}$ and has support only at $x = 0$. Suppose that gluon topology contributes an amount \mathcal{C} to the flavour-singlet axial charge $g_A^{(0)}$. The flavour-singlet axial charge which is extracted from a polarised deep inelastic experiment is $(g_A^{(0)} - \mathcal{C})$. In contrast, elastic Z^0 exchange processes such as νp elastic scattering [60] and parity violation in light atoms [61, 62] measure the full $g_A^{(0)}$ [52]. One can, in principle, measure the topology term \mathcal{C} by comparing the flavour-singlet axial charges which are extracted from polarised deep inelastic and νp elastic scattering experiments.

If some fraction of the spin of the constituent quark is carried by gluon topology in QCD, then the constituent quark model predictions for $g_A^{(0)}$ are not necessarily in contradiction with the small value of $(g_A^{(0)} - \mathcal{C})$ which is extracted from deep inelastic scattering experiments. The Ellis-Jaffe conjecture [45] ($g_A^{(8)} \simeq g_A^{(0)}|_{\text{inv}}$) may hold in constituent quark models and in QCD but fail if we consider only the partonic ($x > 0$) contributions to the nucleon's axial-charges.⁴

In the absence of the topological term ($\mathcal{C} = 0$), the small value of $g_A^{(0)}$ extracted from polarised deep inelastic scattering would be consistent with the semi-classical predictions for Σ if Δg_{parton} is both large and positive ($\sim +1.5$ at $Q^2 \simeq 1\text{GeV}^2$). At the same time, such a large Δg_{parton} would pose a challenge for constituent quark models, which do not naturally include such an effect. The size of Δg_{parton} is one of the key issues in QCD spin physics at the present time — see Section 6.3.

3.4 Chiral symmetry and $g_A^{(k)}$

We have seen in Sections 3.1-3.3 that the axial charges $g_A^{(k)}$ measure the partonic spin structure of the nucleon. The isotriplet Goldberger-Treiman relation [65]

$$2mg_A^{(3)} = f_\pi g_{\pi NN} \quad (23)$$

relates $g_A^{(3)}$ and therefore $(\Delta u - \Delta d)$ to the product of the pion decay constant f_π and the pion-nucleon coupling constant $g_{\pi NN}$. This result is non-trivial. It means that the spin structure of the nucleon measured in high-energy, high Q^2 polarised deep inelastic scattering is intimately related to spontaneous chiral symmetry breaking and low-energy pion physics.

⁴ Possible $\delta(x)$ terms in deep inelastic structure functions have also been discussed within the context of Regge theory where they are induced by Regge fixed poles with non-polynomial residue [64].

Isosinglet extensions of the Goldberger-Treiman relation are quite subtle because of the $U_A(1)$ problem whereby gluonic degrees of freedom mix with the flavour-singlet Goldstone state to increase the masses of the η and η' mesons [66]. If we work in the approximation $m_u = m_d$, then the $\eta - \eta'$ mass matrix becomes [67]

$$M_{\eta-\eta'}^2 = \begin{pmatrix} \frac{4}{3}m_K^2 - \frac{1}{3}m_\pi^2 & -\frac{2}{3}\sqrt{2}(m_K^2 - m_\pi^2) \\ -\frac{2}{3}\sqrt{2}(m_K^2 - m_\pi^2) & \frac{2}{3}m_K^2 + \frac{1}{3}m_\pi^2 + \chi(0)/N_c \end{pmatrix}. \quad (24)$$

Here we work in the (λ_8, λ_0) basis. The gluonic contribution to the mass of the flavour singlet state is $\chi(0)/N_c$ where $\chi(0)$ is the topological susceptibility [67, 68] and N_c is the number of colours in QCD. We diagonalise the matrix (24) to obtain the masses of the physical η and η' mesons:

$$m_{\eta',\eta}^2 = (m_K^2 + \chi(0)/2N_c) \pm \frac{1}{2}\sqrt{(2m_K^2 - 2m_\pi^2 - \chi(0)/3N_c)^2 + \frac{8}{9}\chi(0)/N_c^2}. \quad (25)$$

If we turn off the gluon mixing term, then one finds $m_{\eta'} = \sqrt{2m_K^2 - m_\pi^2}$ and $m_\eta = m_\pi$. The best fit to the η and η' masses from the quadratic mass formula (25) is $m_\eta = 499\text{MeV}$ and $m_{\eta'} = 984\text{MeV}$ corresponding to taking $\chi(0)/N_c = 0.73\text{GeV}^2$ and an $\eta - \eta'$ mixing angle $\theta \simeq 18.2$ degrees. The physical masses are $m_\eta = 547\text{MeV}$ and $m_{\eta'} = 958\text{MeV}$. Several explanations of the $U_A(1)$ problem and the dynamical origin of the $\chi(0)/N_c$ term have been proposed based on instantons [69, 70] and large N_c arguments [68, 71]. The axial anomaly is central to each of these explanations.

Working in the chiral limit, Shore and Veneziano [26] have used the low-energy $U_A(1)$ effective action of QCD to derive the flavour-singlet Goldberger-Treiman relation

$$2mg_A^{(0)} = \sqrt{\chi'(0)}g_{\phi_0 NN}. \quad (26)$$

Here ϕ_0 is the flavour-singlet Goldstone boson which would exist in a gedanken world where OZI is exact — for example, taking N_c to infinity in Eqs.(24,25) with $\chi(0)$ held constant as a function of N_c [68]. The ϕ_0 is a theoretical object and not a physical state in the spectrum. $\chi'(0)$ is the first derivative of the topological susceptibility. viz.

$$\chi'(0) = \lim_{k^2 \rightarrow 0} \frac{d}{dk^2} \left(\int dz e^{ik \cdot z} i \langle \text{vac} | TQ(z)Q(0) | \text{vac} \rangle \right) \quad (27)$$

where $Q(z) = \frac{\alpha_s}{2\pi} G_{\mu\nu} \tilde{G}^{\mu\nu}(z)$ is the topological charge density. The value of $g_A^{(0)}$ which appears in the flavour-singlet Goldberger-Treiman relation (26) includes any contribution from gluon topology at Bjorken x equal to zero.

The important feature of Eq.(26) is that $g_A^{(0)}$ factorises into the product of the target dependent coupling $g_{\phi_0 NN}$ and the target independent susceptibility term $\sqrt{\chi'(0)}$. The scale dependence of $g_A^{(0)}$ is carried by $\sqrt{\chi'(0)}$; the coupling $g_{\phi_0 NN}$ is

scale independent. Motivated by this observation, Narison, Shore and Veneziano [27] conjectured that any OZI violation in $g_A^{(0)}|_{\text{inv}}$ might be carried by the target independent factor $\sqrt{\chi'(0)}$ and that $g_{\phi_0 NN}$ might be free of significant OZI violation. In a different approach, Brodsky, Ellis and Karliner [72] have used a particular version of the Skyrme model to argue that $g_{\phi_0 NN}$ might be OZI suppressed. The target (in-)dependence of the OZI violation in $(g_A^{(0)} - \mathcal{C})$ may be tested in semi-inclusive measurements of polarised deep inelastic scattering in the target fragmentation region [73]. These experiments [74] could be performed with a polarised proton beam at HERA [75].

The flavour-singlet Goldberger-Treiman relation (26) can also be written as the sum of two terms involving the coupling of the physical η' and a pseudoscalar “glueball” object, G , to the nucleon [26]:

$$2mg_A^{(0)} = Fg_{\eta' NN} + \frac{1}{2f}F^2m_{\eta'}^2g_{G NN} \quad (28)$$

Here F is a scale invariant decay constant [26] and $f = 3$ is the number of light flavours. The coupling $g_{\eta' NN}$ will be measured at ELSA in Bonn.

The flavour-singlet $U_A(1)$ Goldberger-Treiman relation means that the flavour-singlet spin structure of the nucleon is intimately related to gluodynamics and axial $U_A(1)$ symmetry. The phenomenology of $U_A(1)$ dynamics will be explored in several new and ongoing experiments studying η and η' physics. Photo- and leptonproduction of η and η' mesons near threshold is being studied at ELSA [76] and MAMI [77]. Higher energy measurements will be made at CEBAF [78] and HERA [79]. CELSIUS [80] and COSY [81] are studying η and η' production in pp and pn scattering near threshold. Central production of η and η' mesons in pp interactions at 450 GeV/c has been measured [82] by the WA102 Collaboration at CERN. CLEO has measured the hard form-factors for the processes $\eta \rightarrow \gamma\gamma^*$ and $\eta' \rightarrow \gamma\gamma^*$ [83]. They have also observed strikingly large branching ratios for B decays into an η' and additional hadrons [84]⁵ which may [85] be related to the axial anomaly. When combined with polarised deep inelastic scattering, these experiments on η and η' production and decay, provide complementary windows on the role of gluons in dynamical chiral symmetry breaking.

We now review the theory of the axial anomaly and its relation to the first moment of g_1 .

⁵ One finds $\mathcal{B}(B \rightarrow \eta' X) = (6.2 \pm 1.6 \pm 1.3) \times 10^{-4}$ under the constraint $2.0 < p_{\eta'} < 2.7 \text{ GeV}/c$ [84]. Exclusive $B \rightarrow \eta' K$ decays have been observed with branching ratios $\mathcal{B}(B^+ \rightarrow \eta' K^+) = (6.5^{+1.5}_{-1.4} \pm 0.9) \times 10^{-5}$ and $\mathcal{B}(B^0 \rightarrow \eta' K^0) = (4.7^{+2.7}_{-2.0} \pm 0.9) \times 10^{-5}$.

4 The axial anomaly

In QCD one has to consider the effect of renormalisation. The flavour singlet axial vector current $J_{\mu 5}^{GI}$ in Eqs.(10,11) satisfies the anomalous divergence equation [17, 18]

$$\partial^\mu J_{\mu 5}^{GI} = 2f\partial^\mu K_\mu + \sum_{i=1}^f 2im_i \bar{q}_i \gamma_5 q_i \quad (29)$$

where

$$K_\mu = \frac{g^2}{16\pi^2} \epsilon_{\mu\nu\rho\sigma} \left[A_a^\nu \left(\partial^\rho A_a^\sigma - \frac{1}{3} g f_{abc} A_b^\rho A_c^\sigma \right) \right] \quad (30)$$

is a renormalised version of the gluonic Chern-Simons current and the number of light flavours f is 3. Eq.(29) allows us to write

$$J_{\mu 5}^{GI} = J_{\mu 5}^{\text{con}} + 2fK_\mu \quad (31)$$

where $J_{\mu 5}^{\text{con}}$ and K_μ satisfy the divergence equations

$$\partial^\mu J_{\mu 5}^{\text{con}} = \sum_{i=1}^f 2im_i \bar{q}_i \gamma_5 q_i \quad (32)$$

and

$$\partial^\mu K_\mu = \frac{g^2}{8\pi^2} G_{\mu\nu} \tilde{G}^{\mu\nu}. \quad (33)$$

Here $\frac{g^2}{8\pi^2} G_{\mu\nu} \tilde{G}^{\mu\nu}$ is the topological charge density. The partially conserved current is scale invariant and the scale dependence of $J_{\mu 5}^{GI}$ is carried entirely by K_μ . When we make a gauge transformation U the gluon field transforms as

$$A_\mu \rightarrow U A_\mu U^{-1} + \frac{i}{g} (\partial_\mu U) U^{-1} \quad (34)$$

and the operator K_μ transforms as

$$K_\mu \rightarrow K_\mu + i \frac{g}{16\pi^2} \epsilon_{\mu\nu\alpha\beta} \partial^\nu \left(U^\dagger \partial^\alpha U A^\beta \right) + \frac{1}{96\pi^2} \epsilon_{\mu\nu\alpha\beta} \left[(U^\dagger \partial^\nu U) (U^\dagger \partial^\alpha U) (U^\dagger \partial^\beta U) \right]. \quad (35)$$

Gauge transformations shuffle a scale invariant operator quantity between the two operators $J_{\mu 5}^{\text{con}}$ and K_μ whilst keeping $J_{\mu 5}^{GI}$ invariant.

The nucleon matrix element of $J_{\mu 5}^{GI}$ is

$$\langle p, s | J_{5\mu}^{GI} | p', s' \rangle = 2m \left[\tilde{s}_\mu G_A(l^2) + l_\mu \tilde{s} G_P(l^2) \right] \quad (36)$$

where $l_\mu = (p' - p)_\mu$ and $\tilde{s}_\mu = \bar{u}_{(p,s)} \gamma_\mu \gamma_5 u_{(p',s')} / 2m$. Since $J_{5\mu}^{GI}$ does not couple to a massless Goldstone boson it follows that $G_A(l^2)$ and $G_P(l^2)$ contain no massless pole terms. The forward matrix element of $J_{5\mu}^{GI}$ is well defined and

$$g_A^{(0)}|_{\text{inv}} = E(\alpha_s) G_A(0). \quad (37)$$

We would like to isolate the gluonic contribution to $G_A(0)$ associated with K_μ and thus write $g_A^{(0)}$ as the sum of “quark” and “gluonic” contributions. Here one has to be careful because of the gauge dependence of the operator K_μ . To understand the gluonic contributions to $g_A^{(0)}$ it is helpful to go back to the deep inelastic cross-section in Section 2.1.

4.1 The anomaly and the first moment of g_1

Working in the target rest frame, the spin dependent part of the deep inelastic cross-section, Eq.(6), is given by

$$\frac{d^2\sigma}{d\Omega dE'} = \frac{\alpha^2}{Q^4} \frac{E'}{E} L_{\mu\nu}^A W_A^{\mu\nu} \quad (38)$$

where the lepton tensor

$$L_{\mu\nu}^A = 2i\epsilon_{\mu\nu\alpha\beta} k^\alpha q^\beta \quad (39)$$

describes the lepton-photon vertex and the hadronic tensor

$$\frac{1}{2m} W_A^{\mu\nu} = i\epsilon^{\mu\nu\rho\sigma} q_\rho \left(s_\sigma \frac{1}{p \cdot q} g_1(x, Q^2) + [p \cdot q s_\sigma - s \cdot q p_\sigma] \frac{1}{m^2 p \cdot q} g_2(x, Q^2) \right) \quad (40)$$

describes the photon-nucleon interaction.

Deep inelastic scattering involves the Bjorken limit: $Q^2 = -q^2$ and $p \cdot q$ both $\rightarrow \infty$ with $x = \frac{Q^2}{2p \cdot q}$ held fixed. In terms of light-cone coordinates this corresponds to taking $q_- \rightarrow \infty$ with $q_+ = -xp_+$ held finite. The leading term in $W_A^{\mu\nu}$ is obtained by taking the Lorentz index of s_σ as $\sigma = +$. (Other terms are suppressed by powers of $\frac{1}{q_-}$.)

The flavour-singlet axial charge which is measured in the first moment of g_1 is given by the matrix element

$$2ms_\mu g_A^{(0)} = \langle p, s | J_{\mu 5}^{GI} | p, s \rangle_c. \quad (41)$$

If we wish to understand the first moment of g_1 in terms of the matrix elements of anomalous currents ($J_{\mu 5}^{\text{con}}$ and K_μ), then we have to understand the forward matrix element of K_+ .

Here we are fortunate in that the parton model is formulated in the light-cone gauge ($A_+ = 0$) where the forward matrix elements of K_+ are invariant. In the light-cone gauge the non-abelian three-gluon part of K_+ vanishes. The forward matrix elements of K_+ are then invariant under all residual gauge degrees of freedom. Furthermore, in this gauge, K_+ measures the gluonic “spin” content of the polarised target [86, 87]. We find [22, 24]

$$G_A^{(A_+=0)}(0) = \sum_q \Delta q_{\text{con}} - f \frac{\alpha_s}{2\pi} \Delta g \quad (42)$$

where Δq_{con} is measured by the partially conserved current J_{+5}^{con} and $-\frac{\alpha_s}{2\pi}\Delta g$ is measured by K_+ . The gluonic term in Eq.(42) offers a possible source for any OZI violation in $g_A^{(0)}|_{\text{inv}}$.

What is the relation between the formal decomposition in Eq.(42) and our previous (more physical) expression (22) ?

4.2 Questions of gauge invariance

In perturbative QCD Δq_{con} is identified with Δq_{parton} and Δg is identified with Δg_{parton} — see Section 6.1 below. If we were to work only in the light-cone gauge we might think that we have a complete parton model description of the first moment of g_1 . However, one is free to work in any gauge including a covariant gauge where the forward matrix elements of K_+ are not necessarily invariant under the residual gauge degrees of freedom [25].

We illustrate this by an example in covariant gauge.

The matrix elements of K_μ need to be specified with respect to a specific gauge. In a covariant gauge we can write

$$\langle p, s | K_\mu | p', s' \rangle_c = 2m \left[\tilde{s}_\mu K_A(l^2) + l_\mu l \cdot \tilde{s} K_P(l^2) \right] \quad (43)$$

where K_P contains a massless Kogut-Susskind pole [88]. This massless pole cancels with a corresponding massless pole term in $(G_P - K_P)$. In an axial gauge $n \cdot A = 0$ the matrix elements of the gauge dependent operator K_μ will also contain terms proportional to the gauge fixing vector n_μ .

We may define a gauge-invariant form-factor $\chi^g(l^2)$ for the topological charge density (33) in the divergence of K_μ :

$$2ml \cdot \tilde{s} \chi^g(l^2) = \langle p, s | \frac{g^2}{8\pi^2} G_{\mu\nu} \tilde{G}^{\mu\nu} | p', s' \rangle_c. \quad (44)$$

Working in a covariant gauge, we find

$$\chi^g(l^2) = K_A(l^2) + l^2 K_P(l^2) \quad (45)$$

by contracting Eq.(43) with l^μ .

When we make a gauge transformation any change δ_{gt} in $K_A(0)$ is compensated by a corresponding change in the residue of the Kogut-Susskind pole in K_P , viz.

$$\delta_{\text{gt}}[K_A(0)] + \lim_{l^2 \rightarrow 0} \delta_{\text{gt}}[l^2 K_P(l^2)] = 0. \quad (46)$$

The Kogut-Susskind pole corresponds to the Goldstone boson associated with spontaneously broken $U_A(1)$ symmetry [15]. There is no Kogut-Susskind pole in perturbative QCD. It follows that the quantity which is shuffled between the J_{+5}^{con} and K_+

contributions to $g_A^{(0)}$ is strictly non-perturbative; it vanishes in perturbative QCD and is not present in the QCD parton model.

One can show [25, 89] that the forward matrix elements of K_μ are invariant under “small” gauge transformations (which are topologically deformable to the identity) but not invariant under “large” gauge transformations which change the topological winding number. Perturbative QCD involves only “small” gauge transformations; “large” gauge transformations involve strictly non-perturbative physics. The second term on the right hand side of Eq.(35) is a total derivative; its matrix elements vanish in the forward direction. The third term on the right hand side of Eq.(35) is associated with the gluon topology [89].

The topological winding number is determined by the gluonic boundary conditions at “infinity” ⁶ [14, 15]. It is insensitive to local deformations of the gluon field $A_\mu(z)$ or of the gauge transformation $U(z)$. When we take the Fourier transform to momentum space the topological structure induces a light-cone zero-mode which can contribute to g_1 only at $x = 0$. Hence, we are led to consider the possibility that there may be a term in g_1 which is proportional to $\delta(x)$ [19].

It remains an open question whether the net non-perturbative quantity which is shuffled between $K_A(0)$ and $(G_A - K_A)(0)$ under “large” gauge transformations is finite or not. If it is finite and, therefore, physical, then, when we choose $A_+ = 0$, this non-perturbative quantity must be contained in some combination of the Δq_{con} and Δg in Eq.(42).

5 Gluon topology and $g_A^{(0)}$

We now explain how tunneling processes may induce topological polarisation inside a nucleon. This effect is related to the realisation of $U_A(1)$ symmetry breaking [15, 69, 70] by instantons.

5.1 $U_A(1)$ symmetry

In classical field theory Noether’s theorem tells us that there is a conserved current associated with each global symmetry of the Lagrangian. Chiral $SU(2)_L \otimes SU(2)_R$ is associated with the isotriplet axial vector current $J_{\mu 5}^{(3)}$. In the classical version of QCD (before we turn on vacuum polarisation) the chiral singlet $U_A(1)$ or $U(1)_L \otimes U(1)_R$ symmetry of \mathcal{L}_{QCD} is associated with the Noether current

$$\mathcal{N}_{\mu 5} = \left(\bar{u} \gamma_\mu \gamma_5 u + \bar{d} \gamma_\mu \gamma_5 d + \bar{s} \gamma_\mu \gamma_5 s \right)_{\text{Noether}}. \quad (47)$$

⁶A large surface with boundary which is spacelike with respect to the positions z_k of any operators or fields in the physical problem.

This classical current satisfies the divergence equation

$$\partial^\mu \mathcal{N}_{\mu 5} = \sum_{i=1}^f 2im_i \bar{q}_i \gamma_5 q_i. \quad (48)$$

$\mathcal{N}_{\mu 5}$ is gauge invariant; there is no anomaly in this classical theory. The classical theory predicts the existence of the flavour-singlet, pseudoscalar Goldstone boson ϕ_0 which we introduced in Section 3.4. The axial anomaly and the absence of any such boson in the physical spectrum means that the realisation of $U_A(1)$ symmetry in real QCD (with interactions) is quite subtle.

We choose $A_0 = 0$ gauge and define two operator charges:

$$X(t) = \int d^3z J_{05}^{GI}(z) \quad (49)$$

and

$$Q_5(t) = \int d^3z J_{05}^{\text{con}}(z) \quad (50)$$

corresponding to the gauge-invariant and partially conserved axial-vector currents respectively.

The charge $X(t)$ is manifestly gauge invariant whereas Q_5 is only invariant under “small” gauge transformations. It transforms as

$$Q_5 \rightarrow Q_5 - 2n \quad (51)$$

where n is the winding number associated with the gauge transformation U . Whilst Q_5 is gauge dependent, we can define a gauge invariant Q_5 chirality, \mathcal{Q}_5 , of any given operator \mathcal{O} through the gauge-invariant eigenstates of the commutator

$$[Q_5, \mathcal{O}]_- = \mathcal{Q}_5 \mathcal{O}. \quad (52)$$

The gluon field operator and its derivative have zero Q_5 chirality and non-zero $X(t)$ chirality [90].

5.2 Instantons and $U_A(1)$ symmetry

When topological effects are taken into account, the QCD vacuum $|\theta\rangle$ is a coherent superposition

$$|\theta\rangle = \sum_m e^{im\theta} |m\rangle \quad (53)$$

of the eigenstates $|m\rangle$ of $\int d\sigma_\mu K^\mu \neq 0$ [14, 91]. Here σ_μ is a large surface which is defined [91] such that its boundary is spacelike with respect to the positions z_k of any operators or fields in the physical problem under discussion. For integer values of the topological winding number m , the states $|m\rangle$ contain mf quark-antiquark pairs with non-zero Q_5 chirality $\sum_l \chi_l = -2\xi_R f m$ where f is the number of light-quark flavours. Relative to the $|m=0\rangle$ state, the $|m=+1\rangle$ state carries topological

winding number +1 and f quark-antiquark pairs with Q_5 chirality equal to $-2f\xi_R$. The factor ξ_R is equal to +1 if the $U_A(1)$ symmetry of QCD is associated with $J_{\mu 5}^{\text{con}}$ and equal to -1 if the $U_A(1)$ symmetry is associated with $J_{\mu 5}^{GI}$ — see below.

There are two schools of thought [15, 70] about how instantons break $U_A(1)$ symmetry. Both of these schools start from 't Hooft's observation [69] that the flavour determinant

$$\langle \det \left[\bar{q}_L^i q_R^j(z) \right] \rangle_{\text{inst.}} \neq 0 \quad (54)$$

in the presence of a vacuum tunneling process between states with different topological winding number. (We denote the tunneling process by the subscript “inst.”. It is not specified at this stage whether “inst.” denotes an instanton or an anti-instanton.)

(a) **Explicit $U_A(1)$ symmetry breaking**

In this scenario [69, 70] the $U_A(1)$ symmetry of QCD is associated with the current $J_{\mu 5}^{GI}$ and the topological charge density is treated like a mass term in the divergence of $J_{\mu 5}^{GI}$. The quark chiralities which appear in the flavour determinant (54) are associated with $X(t)$ so that the net axial charge $g_A^{(0)}$ is not conserved ($\Delta X \neq 0$) and the net Q_5 chirality is conserved ($\Delta Q_5 = 0$) in quark instanton scattering processes.

In QCD with f light flavoured quarks the (anti-)instanton “vertex” involves a total of $2f$ light quarks and antiquarks. Consider a flavour-singlet combination of f right-handed ($Q_5 = +1$) quarks incident on an anti-instanton. The final state for this process consists of a flavour-singlet combination of f left-handed ($Q_5 = -1$) quarks; $+2f$ units of Q_5 chirality are taken away by an effective “schizon” [70] which carries zero energy and zero momentum. The “schizon” is introduced to ensure Q_5 conservation. Energy and momentum are conserved between the in-state and out-state quarks in the quark-instanton scattering process. The non-conservation of $g_A^{(0)}$ is ensured by a term coupled to K_μ with equal magnitude and opposite sign to the “schizon” term which also carries zero energy and zero momentum. This gluonic term describes the change in the topological winding number which is induced by the tunneling process. The anti-instanton changes the net $U_A(1)$ chirality by an amount ($\Delta X = -2f$).

This picture is the basis of 't Hooft's effective instanton interaction [69].

(b) **Spontaneous $U_A(1)$ symmetry breaking**

In this scenario the $U_A(1)$ symmetry of QCD is associated with the partially-conserved axial-vector current $J_{\mu 5}^{\text{con}}$. Here, the quark chiralities which appear in the flavour determinant (54) are identified with Q_5 . With this identification, the net axial charge $g_A^{(0)}$ is conserved ($\Delta X = 0$) and the net Q_5 chirality is

not conserved ($\Delta Q_5 \neq 0$) in quark instanton scattering processes. This result is the opposite to what happens in the explicit symmetry breaking scenario. When f right-handed quarks scatter on an instanton⁷ the final state involves f left-handed quarks. There is no “schizon” and the instanton induces a change in the net Q_5 chirality $\Delta Q_5 = -2f$. The conservation of $g_A^{(0)}$ is ensured by the gluonic term coupled to K_μ which measures the change in the topological winding number and which carries zero energy and zero momentum. The charge Q_5 is time independent for massless quarks (where $J_{\mu 5}^{\text{con}}$ is conserved). Since $\Delta Q_5 \neq 0$ in quark instanton scattering processes we find that the $U_A(1)$ symmetry is spontaneously broken by instantons. The Goldstone boson is manifest [15] as the massless Kogut-Susskind pole which couples to $J_{\mu 5}^{\text{con}}$ and K_μ but not to $J_{\mu 5}^{GI}$ — see Eq.(43).

It is important to note that the $X(t)$ and Q_5 chiralities have different physical content. The difference between the two theories of quark instanton interactions is about more than just the sign of the (X or Q_5) chirality which is flipped in the quark instanton scattering process. We now explain why these two possible realisations of $U_A(1)$ symmetry breaking have a different signature in νp elastic scattering.

5.3 The topological contribution to $g_A^{(0)}$

In both the explicit and spontaneous symmetry breaking scenarios we may consider multiple scattering of the incident quark first from an instanton and then from an anti-instanton. Let this process recur a large number of times. When we time-average over a large number of such interactions, then the time averaged expectation value of the chirality Q_5 carried by the incident quark is reduced from the naive value +1 that it would take in the absence of vacuum tunneling processes. Indeed, in one flavour QCD the time averaged value of Q_5 tends to zero at large times [29, 30].

In the spontaneous $U_A(1)$ symmetry breaking scenario [15] any instanton induced suppression of the flavour-singlet axial charge which is measured in polarised deep inelastic scattering is compensated by a net transfer of axial charge or “spin” from partons carrying finite momentum fraction x to the flavour-singlet topological term at $x = 0$. It induces a flavour-singlet $\delta(x)$ term in g_1 which is not present in the explicit $U_A(1)$ symmetry breaking scenario.

The net topological term is gauge invariant. In the $A_0 = 0$ gauge the $x = 0$ polarisation is “gluonic” and is measured by $\int d^3z K_0$. In the light-cone gauge this polarisation may be re-distributed between the “quark” and “gluonic” terms measured by J_{+5}^{con} and K_+ respectively.

To guide our intuition about non-perturbative QCD it is sometimes helpful to consider analogies with similar phenomena in condensed matter physics. For exam-

⁷cf. an anti-instanton in the explicit $U_A(1)$ symmetry breaking scenario.

ple, the Nambu-Jona-Lasino (NJL) model [16, 12, 13] is motivated by the analogy between the constituent quarks and the Dirac quasi-particles which appear in the BCS theory of superconductivity [92]. Keeping in mind that the underlying physics is fundamentally different, it is nevertheless interesting to note that polarised zero-momentum modes are observed in low temperature physics in the form of polarised condensates. The vacuum of the A-phase of superfluid ^3He behaves both as an orbital ferromagnet and uniaxial liquid crystal with spontaneous magnetisation along the anisotropy axis \hat{l} , and as a spin antiferromagnet with magnetic anisotropy along a second axis \hat{d} [93]. Recent experiments [94] have revealed that superfluidity in ^4He can form in finite systems; 60 atoms of ^4He are the minimum needed for superfluidity.

5.4 How to measure topological polarisation

The scale-invariant flavour singlet axial charge can be measured independently in elastic Z^0 exchange processes such as elastic neutrino proton scattering [60] and parity violation in light atoms [61, 62]. QCD renormalisation group arguments tell us that the neutral current axial charge which is measured in elastic νp scattering is [52]

$$\begin{aligned} g_A^{(Z)} &= \frac{1}{2} g_A^{(3)} + \frac{1}{6} g_A^{(8)} - \frac{1}{6} (1 + C) g_A^{(0)}|_{\text{inv}} + \mathcal{O}\left(\frac{1}{m_h}\right) \\ &= \frac{1}{2} \left(g_A^{(3)} - \Delta s|_{\text{inv}} \right) - \frac{1}{6} C g_A^{(0)}|_{\text{inv}} + \mathcal{O}\left(\frac{1}{m_h}\right). \end{aligned} \quad (55)$$

Here C denotes the leading order heavy-quark contributions to $g_A^{(Z)}$ and m_h represents the heavy-quark mass. Numerically, C is a $\simeq 6 - 10\%$ correction [52] — within the present experimental error on $g_A^{(0)}|_{\text{inv}}$. The flavour-singlet axial charge in Eq.(55) includes any contribution from the topological term at $x = 0$ ⁸. (In νp elastic scattering there is no kinematic factor which could filter out zero mode contributions to $g_A^{(0)}$, unlike deep inelastic scattering where Bjorken $x = 0$ is kinematically unreachable at finite Q^2 .)

If the topological contribution \mathcal{C} to $g_A^{(0)}$ is finite, then the flavour-singlet axial charge which is extracted from a polarised deep inelastic experiment is $(g_A^{(0)} - \mathcal{C})$. Elastic Z^0 exchange processes such as νp elastic scattering [60] and parity violation in light atoms [61, 62] measure the full $g_A^{(0)}$ [52]. One can measure the effect of the topological $x = 0$ polarisation by comparing the flavour-singlet axial charges which are extracted from polarised deep inelastic and νp elastic scattering experiments.

⁸ Heavy-quark instanton interactions are suppressed as $\mathcal{O}(1/m_h)$ where m_h is the heavy-quark mass [95]. It follows that the coefficient of any heavy-quark $\delta(x)$ term in g_1 decouples as $\mathcal{O}(1/m_h)$. It does not affect the relation between polarised deep inelastic scattering and νp elastic scattering.

6 Partons and g_1

6.1 The QCD parton model

The parton model description of polarised deep inelastic scattering involves writing the deep inelastic structure functions as the sum over the convolution of “soft” quark and gluon parton distributions with “hard” photon-parton scattering coefficients. We focus on the flavour-singlet part of g_1

$$g_1|_{\text{singlet}} = \frac{1}{9} \left(\sum_q \Delta q \otimes C^q + N_f \Delta g \otimes C^g \right). \quad (56)$$

Here, $\Delta q(x)$ and $\Delta g(x)$ denote the quark and gluon parton distributions, C^q and C^g denote the corresponding hard scattering coefficients, and N_f is the number of quark flavours liberated into the final state. The parton distributions are target dependent and describe a flux of quark and gluon partons into the hard (target independent) photon-parton interaction which is described by the coefficients. The separation of g_1 into “hard” and “soft” is not unique and depends on the choice of factorisation scheme [96, 97, 98, 99].

The hard coefficients are calculable in perturbative QCD. One can use a kinematic cut-off on the partons’ transverse momentum squared ($k_T^2 > \lambda^2$) to define the factorisation scheme and thus separate the hard and soft parts of the phase space for the photon-parton collision. The cut-off λ^2 is called the factorisation scale. The coefficients have the perturbative expansion $C^q = \delta(1-x) + \frac{\alpha_s}{2\pi} f^q(x, Q^2/\lambda^2)$ and $C^g = \frac{\alpha_s}{2\pi} f^g(x, Q^2/\lambda^2)$ where the functions f^q and f^g have at most a $\ln(1-x)$ singularity when $x \rightarrow 1$ [100].

The gluon coefficient is calculated from the box graph for photon-gluon fusion. We use a cut-off on the transverse momentum squared of the struck quark relative to the photon-gluon direction to separate the total phase space into “hard” ($k_T^2 \geq \lambda^2$) and “soft” ($k_T^2 < \lambda^2$) contributions. One finds [101]:

$$\begin{aligned} g_1^{(\gamma^*g)}(x, Q^2, P^2)|_{\text{hard}} = & -\frac{\alpha_s}{2\pi} \frac{\sqrt{1 - \frac{4(m^2 + \lambda^2)}{s}}}{1 - \frac{4x^2 P^2}{Q^2}} \left[(2x-1) \left(1 - \frac{2xP^2}{Q^2} \right) \right. \\ & \left(1 - \frac{1}{\sqrt{1 - \frac{4(m^2 + \lambda^2)}{s}} \sqrt{1 - \frac{4x^2 P^2}{Q^2}}} \ln \left(\frac{1 + \sqrt{1 - \frac{4x^2 P^2}{Q^2}} \sqrt{1 - \frac{4(m^2 + \lambda^2)}{s}}}{1 - \sqrt{1 - \frac{4x^2 P^2}{Q^2}} \sqrt{1 - \frac{4(m^2 + \lambda^2)}{s}}} \right) \right) \\ & \left. + (x-1 + \frac{xP^2}{Q^2}) \frac{(2m^2(1 - \frac{4x^2 P^2}{Q^2}) - P^2 x(2x-1)(1 - \frac{2xP^2}{Q^2}))}{(m^2 + \lambda^2)(1 - \frac{4x^2 P^2}{Q^2}) - P^2 x(x-1 + \frac{xP^2}{Q^2})} \right] \end{aligned} \quad (57)$$

for each flavour of quark liberated into the final state. Here m is the quark mass, $P^2 = -p^2$ is the virtuality of the gluon, x is the Bjorken variable ($x = \frac{Q^2}{2\nu}$) and s is the centre of mass energy squared $s = (p+q)^2 = Q^2(\frac{1-x}{x}) - P^2$ for the photon-gluon collision.

If we set λ^2 to zero, thus including the entire phase space, then we obtain the full box graph contribution to $g_1^{\gamma^*g}$. The gluon structure function $g_1^{(\gamma^*g)}$ is invariant under the exchange of $(p \leftrightarrow q)$. If we take λ^2 to be finite and independent of x , then the crossing symmetry of $g_1^{(\gamma^*g)}$ under the exchange of $(p \leftrightarrow q)$ is realised separately in each of the “hard” and “soft” parts of $g_1^{(\gamma^*g)}$.

When Q^2 is much greater than the other scales (λ^2, m^2, P^2) in Eq.(57) the expression for $g_1^{(\gamma^*g)}$ simplifies to

$$g_1^{(\gamma^*g)}|_{\text{hard}} = \frac{\alpha_s}{2\pi} \left[(2x-1) \left(\ln \frac{Q^2}{\lambda^2} + \ln \frac{1-x}{x} - 1 \right) \right. \\ \left. + (2x-1) \ln \frac{\lambda^2}{x(1-x)P^2 + (m^2 + \lambda^2)} + (1-x) \frac{2m^2 - P^2x(2x-1)}{x(1-x)P^2 + m^2 + \lambda^2} \right]. \quad (58)$$

We choose an x -independent cut-off ($Q^2 \gg \lambda^2, m^2, P^2$). The first moment of $g_1^{(\gamma^*g)}|_{\text{hard}}$ is the sum of two contributions [96]:

$$\int_0^1 dx g_1^{(\gamma^*g)}|_{\text{hard}} = -\frac{\alpha_s}{2\pi} \left[1 + \frac{2m^2}{P^2} \frac{1}{\sqrt{1 + 4(m^2 + \lambda^2)/P^2}} \ln \left(\frac{1 - \sqrt{1 + 4(m^2 + \lambda^2)/P^2}}{1 + \sqrt{1 + 4(m^2 + \lambda^2)/P^2}} \right) \right]. \quad (59)$$

The unity term describes a contact photon-gluon interaction. It comes from the region of phase space where the hard photon scatters on a quark or antiquark carrying transverse momentum squared $k_T^2 \sim Q^2$ [24]. The second term comes from the kinematic region $k_T^2 \sim \mathcal{O}(\lambda^2, P^2, m^2)$. It vanishes when we take the factorisation scale $\lambda^2 \gg P^2, m^2$. The $-\frac{\alpha_s}{2\pi}$ factor in Eq.(59) is the coefficient of Δg_{parton} in Eq.(22) and Δg in Eq.(42).

When we apply the operator product expansion the first term in Eq.(59) corresponds to the gluon matrix element of the anomaly current K_μ . If we remove the cut-off by setting λ^2 equal to zero, then the second term in Eq.(59) is the gluon matrix element of $J_{\mu 5}^{\text{con}}$ [96]. This term is associated with the “soft” quark distribution of the gluon $\Delta q^{(g)}(x, \lambda^2)$. By extending this operator product expansion analysis to the higher moments of $g_1^{\gamma^*g}$, one can show that [102, 33, 103] that the axial anomaly contribution to the *shape* of g_1 at finite x is given by the convolution of the polarised gluon distribution $\Delta g(x, Q^2)$ with the hard coefficient

$$\tilde{C}^{(g)}|_{\text{anom}} = -\frac{\alpha_s}{\pi}(1-x). \quad (60)$$

This anomaly contribution is a small x effect in g_1 ; it is essentially negligible for x less than 0.05 [101, 104, 105, 106]. The hard coefficient $\tilde{C}^{(g)}|_{\text{anom}}$ is normally included as a term in C^g — Eq.(56). It is associated with two-quark jet events carrying $k_T^2 \sim Q^2$ in the final state.

One could also consider an x -dependent cut-off on the struck quark’s virtuality [96, 101]

$$m^2 - k^2 = P^2x + \frac{k_T^2 + m^2}{(1-x)} > \lambda_0^2 = \text{constant}(x) \quad (61)$$

or a cut-off on the invariant mass squared of the quark-antiquark component of the light-cone wavefunction of the target gluon [97, 107]

$$\mathcal{M}_{q\bar{q}}^2 = \frac{k_T^2 + m^2}{x(1-x)} + P^2 \geq \lambda_0^2 = \text{constant}(x). \quad (62)$$

These different choices of infrared cut-offs correspond to different jet definitions and different factorisation schemes for photon-gluon fusion. If we evaluate the first moment of $g_1^{(\gamma^*g)}$ using the cut-off on the quarks' virtuality, then we find “half of the anomaly” in the gluon coefficient through the mixing of transverse and longitudinal momentum components [96, 101]. The anomaly coefficient for the first moment is recovered with the invariant mass squared cut-off through a sensitive cancellation of large and small x contributions [96].

The x -independent cut-off is preferred for discussions of the axial anomaly and the symmetry properties of the γ^*g interaction. The reason for this is that the transverse momentum is defined perpendicular to the plane spanned by p_μ and q_μ in momentum space. The x -dependent cut-offs mix the transverse and longitudinal components of momentum. Substituting Eqs.(61,62) into Eq.(57) we find that the “hard” and “soft” contributions to $g_1^{(\gamma^*g)}$ do not separately satisfy the $(p \leftrightarrow q)$ symmetry of $g_1(x, Q^2)$ if use the x -dependent cut-offs to define the “hard” part of the total phase space [108].

6.2 QCD evolution

In deep inelastic scattering experiments the different x data points on g_1 are each measured at different values of Q^2 , viz. $x_{\text{expt.}}(Q^2)$. One has to evolve these experimental data points to the same value of Q^2 in order to test the Bjorken [44] and Ellis-Jaffe [45] sum-rules.

The structure function g_1 is given by the sum of the convolution of the parton distributions Δq and Δg with the hard scattering coefficients C^q and C^g respectively — see Eq.(56). The structure function is dependent on Q^2 and independent of the factorisation scale λ^2 and the “scheme” used to separate the γ^* -parton cross-section into “hard” and “soft” contributions. Examples of different “schemes” are the transverse momentum squared and virtuality cut-offs that we discussed in Section 6.1.

In the parton model formula (56) the hard coefficients C^q and C^g are calculable in perturbative QCD as a function of Q^2 and the factorisation scale λ^2 . The λ^2 dependence of the parton distributions is given by the DGLAP equations [109]

$$\begin{aligned} \frac{d}{dt} \Delta \Sigma(x, t) &= \frac{\alpha_s(t)}{2\pi} \left[\int_x^1 \frac{dy}{y} \Delta P_{qq}\left(\frac{x}{y}\right) \Delta \Sigma(y, t) + 2N_f \int_x^1 \frac{dy}{y} \Delta P_{qg}\left(\frac{x}{y}\right) \Delta g(y, t) \right] \\ \frac{d}{dt} \Delta g(x, t) &= \frac{\alpha_s(t)}{2\pi} \left[\int_x^1 \frac{dy}{y} \Delta P_{gq}\left(\frac{x}{y}\right) \Delta \Sigma(y, t) + \int_x^1 \frac{dy}{y} \Delta P_{gg}\left(\frac{x}{y}\right) \Delta g(y, t) \right] \end{aligned} \quad (63)$$

where $\Sigma(x, t) = \sum_q \Delta q(x, t)$ and $t = \ln \lambda^2$. The splitting functions P_{ij} in Eq.(63) have been calculated at next-to-leading order by Mertig, Zijlstra and van Neervan [110] and by Vogelsang [111].

6.3 Gluonic contributions to g_1

The size of Δg_{parton} is one of the key issues in QCD spin physics at the present time.

The polarised gluon distribution $\Delta g(x, Q\lambda^2)$ contributes to g_1 through the convolution $\Delta g \otimes C^g$. Depending on the choice of factorisation scheme, the gluonic coefficient C^g has at most a $\ln(1-x)$ singularity when $x \rightarrow 1$. In contrast, the leading term in the quark coefficient C^q is $\delta(1-x)$. The convolution involving C^g has the practical effect that Δg makes a direct contribution to g_1 only at $x < 0.05$ [101, 104, 105, 106].

At the same time, the λ^2 evolution of the flavour-singlet quark distribution involves the polarised gluon distribution $\Delta g(y, \lambda^2)$ at values of y in the range ($x < y < 1$) [109] — see Eq.(63). Thus, through evolution, the polarised gluon distribution is relevant to the shape of g_1 over the complete x range. This result enables one to carry out next-to-leading order QCD fits to polarised deep inelastic data with the hope of extracting some information about Δg_{parton} . Here, one starts with an ansatz for the shape of $\Delta q(x, Q_0^2)$ and $\Delta g(x, Q_0^2)$ at some particular input scale Q_0^2 . The input distributions are evolved to the range of Q^2 covered by the deep inelastic experiments. Finally, one chooses a particular factorisation scheme (see below) and makes a best fit to the g_1 data in terms of the input shape parameters and the scale Q_0^2 .

Several groups have followed this approach [4,104,105,112-117]. Different QCD motivated fits to the polarised deep inelastic data yield values of $\Delta g_{\text{parton}}(Q^2)$ between zero and +2 at $Q^2 = 1\text{GeV}^2$. The value of Δg_{parton} which is extracted from these fits depends strongly on the functional form which is assumed for the input distributions with only small changes in the overall χ^2 for the fits [115] — we refer to De Florian et al. [115] for a nice overview of QCD fits to g_1 data.

Three schemes are commonly used in the analysis of experimental data: the k_T^2 cut-off, $\overline{\text{MS}}$ and AB schemes. These schemes correspond to different procedures for separating the phase space for photon-gluon fusion into “hard” and “soft” contributions.

In the parton model that we discussed in Section 6.1 using the cut-off on the transverse momentum squared, the polarised gluon contribution to the first moment of g_1 is associated with two-quark jet events carrying $k_T^2 \sim Q^2$. The hard coefficient is given by $C_{\text{PM}}^{(g)} = g_1^{(\gamma^*g)}|_{\text{hard}}$ in Eq.(58) with $Q^2 \geq \lambda^2$ and $\lambda^2 \gg P^2, m^2$. This “parton model scheme” is sometimes called the “chiral invariant” (CI) [33] or JET [112] scheme.

Different schemes can be defined relative to this “parton model scheme” by the transformation

$$C^{(g)}\left(x, \frac{Q^2}{\lambda^2}, \alpha_s(\lambda^2)\right) \rightarrow C^{(g)}\left(x, \frac{Q^2}{\lambda^2}, \alpha_s(\lambda^2)\right) - \tilde{C}_{\text{scheme}}^{(g)}\left(x, \alpha_s(\lambda^2)\right) \quad (64)$$

where $\tilde{C}_{\text{scheme}}^{(g)}$ equals $\frac{\alpha_s}{\pi}$ times a polynomial in x . The parton distributions transform under (64) as

$$\begin{aligned} \Delta\Sigma(x, \lambda^2)_{\text{scheme}} &= \Delta\Sigma(x, \lambda^2)_{\text{PM}} + N_f \int_x^1 \frac{dz}{z} \Delta g\left(\frac{x}{z}, \lambda^2\right)_{\text{PM}} \tilde{C}_{\text{scheme}}^{(g)}(z, \alpha_s(\lambda^2)) \\ \Delta g(x, \lambda^2)_{\text{scheme}} &= \Delta g(x, \lambda^2)_{\text{PM}} \end{aligned} \quad (65)$$

so that g_1 is left invariant by the change of scheme. The virtuality and invariant-mass cut-off versions of the parton model that we discussed in Section 6.1 correspond to different choices of scheme.

The $\overline{\text{MS}}$ and AB schemes are defined as follows. In the $\overline{\text{MS}}$ scheme the gluonic hard scattering coefficient is calculated using the operator product expansion with $\overline{\text{MS}}$ renormalisation [118]. One finds [33, 102]:

$$C_{\overline{\text{MS}}}^{(g)} = C_{\text{PM}}^{(g)} + \frac{\alpha_s}{\pi}(1-x). \quad (66)$$

In this scheme $\int_0^1 dx C_{\overline{\text{MS}}}^{(g)} = 0$ so that $\int_0^1 dx \Delta g(x, \lambda^2)$ decouples from $\int_0^1 dx g_1$. This result corresponds to the fact that there is no gauge-invariant twist-two, spin-one, gluonic operator with $J^P = 1^+$ to appear in the operator product expansion for the first moment of g_1 . In the $\overline{\text{MS}}$ scheme the contribution of $\int_0^1 dx \Delta g$ to the first moment of g_1 is included into $\int_0^1 dx \Sigma_{\overline{\text{MS}}}(x, \lambda^2)$. The AB scheme [119] is defined by the formal operation of adding the x -independent term $-\frac{\alpha_s}{2\pi}$ to the $\overline{\text{MS}}$ gluonic coefficient, viz.

$$C_{\text{AB}}^{(g)}(x) = C_{\overline{\text{MS}}}^{(g)} - \frac{\alpha_s}{2\pi}. \quad (67)$$

In both the parton model and AB schemes $\int_0^1 dx C^{(g)} = -\frac{\alpha_s}{2\pi}$. We refer to Cheng [103] and Llewellyn Smith [120] for a critical discussion of these schemes and their application to polarised deep inelastic scattering.

The SMC and SLAC E-154 experiments quote values of Δg for their own data. The SMC values are [4]

$$\Delta g_{\text{parton}} = +0.25_{-0.22}^{+0.29}, \quad \overline{\text{MS}} \text{ scheme} \quad (68)$$

and

$$\Delta g_{\text{parton}} = +0.99_{-0.70}^{+1.17}, \quad \text{AB scheme} \quad (69)$$

in the $\overline{\text{MS}}$ [118] and AB [119] schemes respectively — each at 1GeV^2 : The E-154 values are [117]

$$\Delta g_{\text{parton}} = +1.8_{-1.0}^{+0.7}, \quad \overline{\text{MS}} \text{ scheme} \quad (70)$$

and

$$\Delta g_{\text{parton}} = +0.4^{+1.7}_{-0.9} \quad , \quad \text{AB scheme} \quad (71)$$

— each at 5GeV^2 .

Dedicated experiments have been proposed to measure Δg_{parton} more precisely. The COMPASS [121] and HERMES [122] experiments will measure charm production in polarised deep inelastic scattering; a further experiment is proposed for SLAC [123]. Polarised RHIC [124] will measure prompt photon production in polarised pp collisions through the process $qg \rightarrow q\gamma$, thus enabling a different measurement of Δg_{parton} . In the longer term there is a proposal to polarise the proton beam at HERA [75, 125]. A polarised proton beam at HERA would allow precision measurements of g_1 at small x where it becomes increasingly more sensitive to the polarised gluon distribution and to study the two-quark-jet cross-section associated with the axial anomaly.

7 The shape of g_1

There have been many theoretical papers proposing possible explanations of the small value of $g_A^{(0)}|_{\text{pDIS}}$ extracted from polarised deep inelastic scattering. Besides offering an explanation of the size of $g_A^{(0)}$ it is important to understand how the different possible effects contribute to the shape of g_1 , which contains considerably more information than just the first moment.

Early constituent quark model calculations of the shape of g_1 [130, 131, 132] still provide a reasonable description of the g_1 data in the “valence” region (x greater than about 0.2). More recent quark model calculations [58, 133] include QCD evolution from the Bag “input scale” μ_0^2 to deep inelastic Q^2 . In their next-to-leading order Bag model fits to deep inelastic data Steffens et al. [58] found that the model “input scale” increased corresponding to a change in the coupling $\alpha_s(\mu_0^2)$ from 0.8 to 0.6 when pion cloud corrections were included into the model input.

Semi-inclusive measurements of g_1 will enable us to disentangle the separate $\Delta q_{\text{valence}}(x)$ and $\Delta \bar{q}_{\text{sea}}(x)$ contributions to g_1 [126, 127]. The first semi-inclusive measurements have been published by the SMC [128]; more precise data will soon be available from HERMES.

If the sum of $\Delta u_v = \int_0^1 dx \Delta u_{\text{valence}}(x)$ and $\Delta d_v = \int_0^1 dx \Delta d_{\text{valence}}(x)$ extracted from semi-inclusive measurements of g_1 falls short of the constituent quark model prediction for $g_A^{(0)}$, then the “discrepancy” could be interpreted as a first hint that some of the nucleon’s spin might reside at $x = 0$. (Recall from Section 5 that instanton tunneling processes have the potential to shift some fraction of $g_A^{(0)}$ from valence partons carrying $x > 0$ to the topological term at $x = 0$.) The first semi-inclusive data (from SMC) yield $\Delta u_v = +0.77 \pm 0.10 \pm 0.08$ and $\Delta d_v = -0.52 \pm 0.14 \pm$

0.09. Combining the errors in quadrature we find $\Delta u_v + \Delta d_v = +0.25 \pm 0.21$ (cf. the constituent quark model prediction $g_A^{(0)} \simeq 0.6$) and $\Delta u_v - \Delta d_v = +1.29 \pm 0.21$ (cf. $g_A^{(3)} = 1.267 \pm 0.004$). It will be interesting to see how these results hold up in the light of more accurate data from HERMES.

Wislicki [129] has analysed the polarised semi-inclusive data from SMC and HERMES looking for possible evidence of the axial anomaly at large x . The data shows no evidence of any deviation between the charge parity $C = +1$ and $C = -1$ polarised quark distributions in the “valence” region $x > 0.3$.

Perturbative QCD Counting Rules [134] make predictions for the large x behaviour of g_1 . The small x extrapolation of g_1 data is presently the largest source of experimental error on deep inelastic measurements of the nucleon’s axial charges. The small x extrapolation is usually motivated either by Regge theory or by perturbative QCD arguments.

We now outline what is known about g_1 at large x (Section 7.1) and at small x (Section 7.2). In Section 7.3 we collect this theory and describe how it explains the shape of the measured spin dependent and spin independent isotriplet structure functions as a function of x .

7.1 g_1 at $x \rightarrow 1$

Perturbative QCD counting rules predict that the parton distributions should behave as a power series expansion in $(1 - x)$ when $x \rightarrow 1$ [134]. We use $q^\uparrow(x)$ and $q^\downarrow(x)$ to denote the parton distributions polarised parallel and antiparallel to the polarised proton. One finds [134]

$$q^{\uparrow\downarrow}(x) \rightarrow (1 - x)^{2n-1+\Delta S_z} \quad ; \quad (x \rightarrow 1). \quad (72)$$

Here, n is the number of spectators and ΔS_z is the difference between the polarisation of the struck quark and the polarisation of the target nucleon. When $x \rightarrow 1$ the QCD counting rules predict that the structure functions should be dominated by valence quarks polarised parallel to the spin of the nucleon. The ratio of polarised to unpolarised structure functions should go to one when $x \rightarrow 1$.

7.2 g_1 at small x

The small x extrapolation of g_1 data is important for precise measurements of the nucleon’s axial charges from deep inelastic scattering. The SLAC data [8, 9] has the smallest experimental error in the x range ($0.01 < x < 0.12$). We show these data in Fig.1.

There are several important properties of the g_1 data at small x .

- (a) The magnitude of $g_1^{(p-n)}$ is significantly greater than the magnitude of $g_1^{(p+n)}$ in the measured small x region. This is in contrast to unpolarised deep inelastic scattering where the small x region is dominated by isoscalar pomeron exchange.
- (b) The isosinglet $g_1^{(p+n)}$ is small and consistent with zero in the measured small x range ($0.01 < x < 0.05$). Polarised gluon models [114] predict that $g_1^{(p+n)}$ may become strongly negative at smaller values of x ($\sim 10^{-4}$) but this remains to be checked experimentally.
- (c) Polarised deep inelastic data from CERN and SLAC consistently indicate a strong isotriplet term in g_1 which rises at small x .

We consider the isotriplet part of g_1 in more detail. Combining the proton data from E-143 [8] together with the neutron data from E-154 [9], one finds a good fit [136, 137] to the SLAC data on $g_1^{(p-n)}$:

$$g_1^{(p-n)} \sim (0.14) x^{-\frac{1}{2}} \quad (73)$$

in the x range ($0.01 < x < 0.12$) at $Q^2 \simeq 5\text{GeV}^2$.

Regge theory makes a prediction for the large $s_{\gamma p}$ dependence of the spin dependent and spin independent parts of the total photoproduction ($Q^2 = 0$) cross-section. It is often used to describe the small x behaviour of deep inelastic structure functions (Q^2 larger than about 2GeV^2). The Regge prediction for the isotriplet part of g_1 is [138, 139]

$$g_1^{(p-n)} \sim x^{-\alpha_{a_1}} \quad , \quad (x \rightarrow 0). \quad (74)$$

Here α_{a_1} is the intercept of the a_1 Regge trajectory. If one makes the usual assumption that the a_1 trajectory is a straight line running parallel to the (ρ, ω) trajectories, then one finds $\alpha_{a_1} = -0.4$.

Clearly, Regge theory does not provide a good description of $g_1^{(p-n)}$ in the measured x range ($0.01 < x < 0.12$). At first glance, this result is surprising since Regge theory provides a good description [140] of the NMC measurements [141] of both the isotriplet and isosinglet parts of F_2 in the same small x range ($0.01 < x < 0.1$) at $Q^2 \simeq 5\text{GeV}^2$. In practice, the shape of g_1 at small x is Q^2 dependent. The Q^2 dependence is driven by DGLAP evolution and, at very small x ($\sim 10^{-3}$), by the resummation of $\alpha_s^l \ln^{2l} x$ radiative corrections — see eg. [105, 142, 143].

To understand this evolution, let us define an effective intercept $\tilde{\alpha}_{a_1}(Q^2)$ to describe the small x behaviour of g_1 at finite Q^2 : $g_1^{(p-n)} \sim x^{-\tilde{\alpha}_{a_1}}$. The net Q^2 dependence of $\tilde{\alpha}_{a_1}$ depends strongly on the value of $\tilde{\alpha}_{a_1}$ which is needed to describe the leading twist part of $g_1^{(p-n)}$ at low momentum scales — for example $\mu_0^2 \sim 0.3\text{GeV}^2$. Let $(\Delta u - \Delta d)(x)$ denote the leading twist (=2) part of $g_1^{(p-n)}$. DGLAP evolution of $(\Delta u - \Delta d)(x)$ from μ_0^2 to deep inelastic Q^2 shifts the weight of the distribution

from larger to smaller values of x whilst keeping the area under the curve, $g_A^{(3)}$, constant. QCD evolution has the practical effect of “filling up” the small x region — increasing the value of $\tilde{\alpha}_{a_1}$ with increasing Q^2 . The scale independence of $g_A^{(3)}$ provides an important constraint on the change in $\tilde{\alpha}_{a_1}$ under QCD evolution. The closer that $\tilde{\alpha}_{a_1}(\mu_0^2)$ is to the Regge prediction -0.4, the more that $\tilde{\alpha}_{a_1}(Q^2)$ will grow in order to preserve the area under $(\Delta u - \Delta d)(x)$ when we increase Q^2 to values typical of deep inelastic scattering.

Badelek and Kwiecinski [142] have investigated the effect of DGLAP and $\alpha_s \ln^2 x$ resummation on the small x behaviour of $g_1^{(p-n)}$. They find a good fit to the data using a flat small- x input distribution at $Q_0^2 = 1\text{GeV}^2$. In their optimal NLO QCD fit to polarised deep inelastic data Glück et al. [105] used a rising input at $\mu_0^2 \simeq 0.3\text{GeV}^2$.

The isosinglet part of g_1 is more complicated because of possible gluonic exchanges in the t -channel. There have been several suggestions how the isosinglet part of g_1 should behave at small x based on non-perturbative [144, 145, 146] and perturbative [105, 147, 148, 149] QCD arguments.

7.3 Isotriplet structure functions

To understand the shape of $g_1^{(p-n)}$ it is helpful to compare the isotriplet part of g_1 with the isotriplet part of F_2 (the nucleon’s spin independent structure function).

In the QCD parton model

$$2x(g_1^p - g_1^n) = \frac{1}{3}x \left[(u + \bar{u})^\uparrow - (u + \bar{u})^\downarrow - (d + \bar{d})^\uparrow + (d + \bar{d})^\downarrow \right] \otimes \Delta C_{NS} \quad (75)$$

and

$$(F_2^p - F_2^n) = \frac{1}{3}x \left[(u + \bar{u})^\uparrow + (u + \bar{u})^\downarrow - (d + \bar{d})^\uparrow - (d + \bar{d})^\downarrow \right] \otimes C_{NS}. \quad (76)$$

Here u and d denote the up and down flavoured quark distributions polarised parallel (\uparrow) and antiparallel (\downarrow) to the target proton and ΔC_{NS} and C_{NS} denote the spin-dependent and spin-independent perturbative QCD coefficients [100]⁹. There is no gluonic or pomeron contribution to the isotriplet structure functions $g_1^{(p-n)}$ and $F_2^{(p-n)}$.

In Fig.2 we show the SLAC data [8, 9] on $g_1^{(p-n)}(x)$ together with the NMC measurement [151] of $F_2^{(p-n)}(x)$. The NMC data are quoted at $Q^2 = 4\text{GeV}^2$. Our SLAC data set is obtained by combining the published E-143 data on g_1^p with the

⁹ The coefficients C_{NS} and ΔC_{NS} have the perturbative expansion $\delta(1-x) + \frac{\alpha_s}{2\pi}f(x)$. They are related (in the $\overline{\text{MS}}$ scheme) by [100] $\Delta C_{NS}(x) = C_{NS}(x) - \frac{\alpha_s}{2\pi} \frac{4}{3}(1+x)$. The difference between C_{NS} and ΔC_{NS} makes a non-negligible contribution to the deep inelastic structure functions only at $x < 0.05$.

E-154 data on g_1^n — both at $Q^2 = 5\text{GeV}^2$. We combine the g_1 measurements to produce one $g_1^{(p-n)}$ data point for each x bin listed by the NMC. Clearly, $2xg_1^{(p-n)}$ is greater than $F_2^{(p-n)}$ for $x < 0.4$ in this data (— see also [137, 3]).

Sum-rules for the first moments of $g_1^{(p-n)}$ and the unpolarised structure function $F_2^{(p-n)}/x$ provide important constraints for our understanding of the structure of the nucleon. The Gottfried integral [150]

$$\begin{aligned} I_G &= \int_0^1 dx \left(\frac{F_2^p - F_2^n}{x} \right) \\ &= \frac{1}{3} \int_0^1 dx \left(u_V(x) - d_V(x) \right) + \frac{2}{3} \int_0^1 dx \left(\bar{u}(x) - \bar{d}(x) \right) \end{aligned} \quad (77)$$

measures any SU(2) flavour asymmetry in the sea. The integral I_G has been measured by the NMC in deep inelastic scattering ($I_G = 0.235 \pm 0.026$) [151] and by the Fermilab E-866 NuSea Collaboration in Drell-Yan production ($I_G = 0.267 \pm 0.018$) [152]. Possible explanations of this effect include the pion cloud of the nucleon [153] and the Pauli-principle [154] at work in the nucleon's sea. We refer to Thomas and Melnitchouk [155] for a pedagogical review of the physics involved in understanding the Gottfried integral.

When we convolute the polarised and unpolarised parton distributions with the perturbative coefficients C_{NS} and ΔC_{NS} the difference between the two coefficients makes a negligible contribution to the structure functions at $x > 0.05$ — the bulk of the x range in Fig.2. Dividing $\frac{1}{3}g_A^{(3)}$ by the central values of I_G measured by the NMC and Fermilab E-866 experiments we obtain 1.78 and 1.57 respectively. Whilst the physical values of $g_A^{(3)}$ and I_G differ markedly from the simple SU(6) predictions, it is interesting to observe that the ratio $\frac{1}{3}g_A^{(3)}/I_G$ is consistent with the SU(6) prediction ($2I_{Bj}/I_G = \frac{5}{3}$).

In Fig.3 we plot the ratio $R_{(3)}(x) = 2xg_1^{(p-n)}/F_2^{(p-n)}$. We also plot the SU(6) prediction for $2I_{Bj}/I_G$, together with the result of dividing twice the value of $\frac{1}{6}g_A^{(3)}$ by the central values of the measured Gottfried integral I_G from NMC (top line) and E-866 (bottom line).

There are several observations to make. First, the deep inelastic data is consistent with $R_{(3)}(x) \simeq \frac{5}{3}$ in the x range ($0.02 < x < 0.4$) [137]. At large x the data is consistent with the QCD Counting Rules prediction

$$R_3 \rightarrow 1 \quad , \quad x \rightarrow 1. \quad (78)$$

The data exhibits no evidence of the simple Regge prediction $R_{(3)} \propto x$ when $x \rightarrow 0$ (— say $x < 0.1$). The SMC have recently published their measurements of $R_{(3)}$ down to $x = 0.005$. This new data is consistent with the SLAC measurements and the observation $R_{(3)} \simeq \frac{5}{3}$.

We make some phenomenological observations which may help to understand the relative shapes of the isotriplet parts of g_1 and F_2 . First, the total area under

$g_1^{(p-n)}$ is fixed by the Bjorken sum-rule. Soffer and Teryaev [136] have observed that $\simeq 50\%$ of the Bjorken sum-rule comes from small x ($x < 0.12$) if the shape (68) is extrapolated to $x = 0$. Suppose that we pivot $g_1^{(p-n)}$ about its measured value at $x = 0.12$ and impose the Regge behaviour $\sim x^{+0.4}$ at smaller values of x instead of the observed small x behaviour $\sim x^{-0.5}$. We shall call this the “Regge modified” $g_1^{(p-n)}$. For the “Regge modified” $g_1^{(p-n)}$ the fraction of the total Bjorken sum-rule which comes from x less than 0.12 would be reduced to $\simeq 17\%$. That is, $\simeq 33\%$ of the total Bjorken sum-rule would be shifted to larger values of x .

A priori, one would expect the simple SU(6) prediction for $R_{(3)}$ to come closest to the ratio of the leading twist contribution to the measured structure functions at a value x^* close to $\frac{1}{3}$ *after* the leading twist parton distributions have been evolved to the quark model scale μ_0^2 . QCD evolution shifts the value of x^* to slightly smaller x at deep inelastic Q^2 . Deep inelastic structure functions fall rapidly to zero when $x \rightarrow 1$. Suppose we combine the “Regge modified” $g_1^{(p-n)}$ together with the measured $F_2^{(p-n)}$ data. The resultant “Regge modified” $R_{(3)}$ would considerably exceed the SU(6) prediction $R_{(3)} = \frac{5}{3}$ in the intermediate x region because of the extra area that has been shifted under $g_1^{(p-n)}$ at $x > 0.12$. However, this contains the x range where we would most expect the SU(6) prediction to work (if it is to work at all). In summary, *if* $R_{(3)}$ takes the SU(6) value $\frac{5}{3}$ at some intermediate value x^* and decreases towards one when we increase x greater than x^* , and if $g_1^{(p-n)}$ has a power law behaviour $\sim x^{-\tilde{\alpha}_{a1}}$ at small x , then $g_1^{(p-n)}$ must rise at small x (in contradiction to Regge theory) with $R_{(3)} \sim \frac{5}{3}$ so that $g_1^{(p-n)}$ saturates the Bjorken sum-rule with the physical value of $g_A^{(3)}$.

To summarise this Section, constituent quark model calculations provide a reasonable description of g_1 in the intermediate x region. The soft Regge theory predictions for the small x behaviour of the g_1 spin structure function seem to fail badly at deep inelastic Q^2 . The shape of the measured isotriplet spin structure function $g_1^{(p-n)}$ may be understood in terms of perturbative QCD Counting Rules (at $x > 0.2$) and constituent quark model ideas (in the x range $0.01 < x < 0.2$).

8 Conclusions and Outlook

Relativistic constituent-quark pion coupling models predict $g_A^{(0)}|_{\text{inv}} \simeq g_A^{(8)} \simeq 0.6$. The value of $g_A^{(0)}$ extracted from polarised deep inelastic scattering experiments is $g_A^{(0)}|_{\text{pDIS}} \simeq 0.2 - 0.35$. This result has inspired many theoretical ideas about the internal spin structure of the nucleon. Central to these ideas is the role that the axial anomaly plays in the transition from parton to constituent quark degrees of freedom in low energy QCD.

In QCD some fraction of the spin of the nucleon and of the constituent quark may be carried by gluon topology. If the topological contribution \mathcal{C} is indeed finite, then

the constituent quark model predictions for $g_A^{(0)}$ are not necessarily in contradiction with the small value of $g_A^{(0)}|_{\text{pDIS}} = (g_A^{(0)} - \mathcal{C})$ extracted from polarised deep inelastic scattering.

New experiments will help to further resolve the spin structure of the nucleon and to distinguish between the various theoretical possibilities.

- Semi-inclusive measurements of g_1 in the current fragmentation region (HERMES) will enable more accurate measurements of the valence and sea quark contributions to g_1 . If a polarised proton beam becomes available at HERA it will be possible to extend this programme into the target fragmentation region and to study the target (in-)dependence of the small value of $g_A^{(0)}|_{\text{pDIS}}$.
- Measurements of open charm production in polarised deep inelastic scattering (COMPASS, HERMES and SLAC) will enable a direct measurement of the polarised gluon distribution $\Delta g(x)$ in deep inelastic scattering. A complementary measurement of $\Delta g(x)$ will come from studies of prompt photon production in polarised pp collisions at RHIC. It will be interesting to compare the deep inelastic and polarised pp measurements of Δg_{parton} . A polarised proton beam at HERA would enable us to measure g_1 at small x where it is most sensitive to $\Delta g(x)$ and to study the two-quark-jet cross-section associated with the axial anomaly.
- A precision measurement of νp elastic scattering or parity violation in light atoms would enable us to make an independent determination of $g_A^{(0)}|_{\text{inv}}$. The value of $g_A^{(0)}|_{\text{inv}}$ which is extracted from these elastic Z^0 exchange processes includes any contribution from topological polarisation at $x = 0$ whereas the deep inelastic measurement does not — thus, enabling us to measure the topological term \mathcal{C} .

The physics of the flavour-singlet axial-charge $g_A^{(0)}$ provides a bridge between the internal spin structure of the nucleon and chiral $U_A(1)$ dynamics. When combined with experimental and theoretical studies of the $\eta - \eta'$ system, QCD spin physics offers a new window on the role of gluons in dynamical chiral symmetry breaking.

Acknowledgements:

I thank B. Povh for the invitation to write this review and for his hospitality at the MPI, Heidelberg. Many of the ideas in this review have been developed in fruitful collaboration with M.M. Brisudova, S.J. Brodsky, R.J. Crewther, A. De Roeck, P.V. Landshoff, I. Schmidt, F.M. Steffens and A.W. Thomas. I also thank V.N. Gribov, H. Fritzsche, P. Minkowski, B. Povh, D. Schütte, G.M. Shore and W.

Weise for helpful discussions about the proton spin problem in QCD and constituent quark models, and N. Bianchi, A. Brüll, G. Garvey, M. Moinester, J. Pochodzalla and R. Windmolders for discussions about experimental data.

References

- [1] EMC Collaboration (J Ashman et al.) Phys. Lett. **B206** (1988) 364; Nucl. Phys. **B328** (1989) 1.
- [2] The Spin Muon Collaboration (D. Adams et al.), Phys. Lett. **B396** (1997) 338; (B. Adeva et al.), Phys. Lett. **B412** (1997) 414.
- [3] The Spin Muon Collaboration (B. Adeva et al), Phys. Rev. **D58** (1998) 112001
- [4] The Spin Muon Collaboration (B. Adeva et al.), Phys. Rev. **D58** (1998) 112002.
- [5] The HERMES Collaboration (K. Ackerstaff et al.), Phys. Lett. **B404** (1997) 383;
The HERMES Collaboration (A. Airapetian et al.), Phys. Lett. **B442** (1998) 484.
- [6] The E-130 Collaboration (G. Baum et al.), Phys. Rev. Lett. **51** (1983) 1135.
- [7] The E-142 Collaboration (P.L. Anthony et al.), Phys. Rev. **D54** (1996) 6620.
- [8] The E-143 Collaboration (K. Abe et al.), Phys. Rev. Lett. **74** (1995) 346;
Phys. Rev. **D58** (1998) 112003.
- [9] The E-154 Collaboration (K. Abe et al.), Phys. Rev. Lett. **79** (1997) 26.
- [10] G. Altarelli, Phys. Rep. **81** (1982) 1.
- [11] A.W. Thomas, Adv. Nucl. Phys. **13** (1984) 1.
- [12] U. Vogl and W. Weise, Prog. Part. Nucl. Phys. **27** (1991) 195.
- [13] S.P. Klevansky, Rev. Mod. Phys. **64** (1992) 649.
- [14] C.G. Callan, R.F. Dashen and D.J. Gross, Phys. Lett. **B63** (1976) 334;
R. Jackiw and C. Rebbi, Phys. Rev. Lett. **37** (1976) 172.
- [15] R.J. Crewther, Effects of Topological Charge in Gauge Theories, in Facts and Prospects of Gauge Theories, Schladming, Austria, February 1978, ed. P. Urban, Acta Physica Austriaca Suppl. **19** (1978) 47.
- [16] Y. Nambu and G. Jona-Lasinio, Phys. Rev. **122** (1961) 345.
- [17] S.L. Adler, Phys. Rev. **177** (1969) 2426.
- [18] J.S. Bell and R. Jackiw, Nuovo Cimento **60A** (1969) 47.
- [19] S.D. Bass, Mod. Phys. Lett. **A13** (1998) 791.

- [20] A.W. Schreiber and A.W. Thomas, Phys. Lett. **B215** (1988) 141.
- [21] K. Steininger and W. Weise, Phys. Rev. **D48** (1993) 1433;
K. Suzuki and W. Weise, Nucl. Phys. **A634** (1998) 141.
- [22] A.V. Efremov and O.V. Teryaev, JINR Report E2-88-287 (1988), and in Proceedings of the International Hadron Symposium, Bechyně 1988, eds. J. Fischer et al. (Czechoslovakian Academy of Science, Prague, 1989) p. 302;
A.V. Efremov, J. Soffer and O.V. Teryaev, Nucl. Phys. **346** (1990) 97.
- [23] G. Altarelli and G.G. Ross, Phys. Lett. **B212** (1988) 391.
- [24] R.D. Carlitz, J.C. Collins, and A.H. Mueller, Phys. Lett. **B214** (1988) 229.
- [25] R.L. Jaffe and A. Manohar, Nucl. Phys. **B337** (1990) 509.
- [26] G. Veneziano, Mod. Phys. Lett. **A4** (1989) 1605;
G.M. Shore and G. Veneziano, Nucl. Phys. **B381** (1992) 23.
- [27] S. Narison, G.M. Shore and G. Veneziano, Nucl. Phys. **B433** (1995) 209.
- [28] H. Fritzsch, Phys. Lett. **B229** (1989) 122, *ibid* **B256** (1991) 75.
- [29] S. Forte, Phys. Lett. **B224** (1989) 189; Nucl. Phys. **B331** (1990) 1.
- [30] S. Forte and E.V. Shuryak, Nucl. Phys. **B357** (1991) 153.
- [31] B.L. Ioffe and M. Karliner, Phys. Lett. **B247** (1990) 387.
- [32] G. Altarelli and G. Ridolfi, Nucl. Phys. B (Proc. Suppl.) **39B,C** (1995) 106.
- [33] H.-Y. Cheng, Int. J. Mod. Phys. **A11** (1996) 5109.
- [34] M. Anselmino, A. Efremov and E. Leader, Phys. Rept. **261** (1995) 1.
- [35] R.L. Jaffe, hep-ph/9602236, in Proc. Erice School *The spin structure of the nucleon*, eds. B. Frois and V. Hughes (World Scientific, 1997).
- [36] J. Ellis and M. Karliner, hep-ph/9601280, in Proc. Erice School *The spin structure of the nucleon*, eds. B. Frois and V. Hughes (World Scientific, 1997).
- [37] B. Lampe and E. Reya, hep-ph/9810270.
- [38] G.M. Shore, Zuoz lecture hep-ph/9812354 and Erice lecture hep-ph/9812355.
- [39] S.D. Bass, Mod. Phys. Lett. **A12** (1997) 1051.
- [40] R.G. Roberts, “The structure of the proton” (Cambridge UP, 1990)

- [41] A.M. Cooper-Sarker, R.C.E. Devenish and A. De Roeck, Int J. Mod. Phys. **A13** (1998) 3385.
- [42] The E-143 Collaboration (K. Abe et al.), Phys. Rev. Lett. **76** (1996) 587;
The E-154 Collaboration (K. Abe et al.), Phys. Lett. **B404** (1997) 377;
The SMC Collaboration (B. Adeva et al.), Phys. Lett. **B336** (1994) 125.
- [43] R.L. Jaffe, Comm. Nucl. Part. Phys. **19** (1990) 239.
- [44] J.D. Bjorken, Phys. Rev. **148** (1966) 1467; Phys. Rev. **D1** (1970) 1376.
- [45] J. Ellis and R.L. Jaffe, Phys. Rev. **D9** (1974) 1444; (E) **D10** (1974) 1669.
- [46] J. Kodaira, Nucl. Phys. **B165** (1980) 129.
- [47] S.A. Larin, Phys. Lett. **B334** (1994) 192; *ibid* **B404** (1997) 153.
- [48] The Particle Data Group (C. Caso et al.), Euro. Phys. J. **C3** (1998) 1.
- [49] F.E. Close and R.G. Roberts, Phys. Lett. **B316** (1993) 165.
- [50] P. Minkowski, in Proc. Workshop on *Effective Field Theories of the Standard Model*, Dobogókő, Hungary 1991, ed. U.-G. Meissner (World Scientific, Singapore, 1992).
- [51] R. Köberle and N.K. Nielsen, Phys. Rev. **D8** (1973) 660;
R.J. Crewther, S.-S. Shei and T.-M. Yan, Phys. Rev. **D8** (1973) 3396;
R.J. Crewther and N.K. Nielsen, Nucl. Phys. **B87** (1975) 52.
- [52] D.B. Kaplan and A.V. Manohar, Nucl. Phys. **B310** (1988) 527.
- [53] I thank R.J. Crewther for emphasising this point.
- [54] S.J. Brodsky and F. Schlumpf, Phys. Lett. **B329** (1994) 111.
- [55] W. Koepf, E.M. Henley and S.J. Pollock, Phys. Lett. **B288** (1992) 11.
- [56] M. Glück, E. Reya and A. Vogt, Z Physik **C67** (1995) 433.
- [57] R.L. Jaffe and G.G. Ross, Phys. Lett. **B93** (1980) 313;
A.W. Schreiber, A.I. Signal and A.W. Thomas, Phys. Rev **D44** (1991) 2653.
- [58] F.M. Steffens, H. Holtmann and A.W. Thomas, Phys. Lett. **B358** (1995) 139.
- [59] V.N. Gribov, Physica Scripta **T15** (1987) 164;
Lund preprint LU-TP-91-7 (1991) unpublished.
- [60] G.T. Garvey, W.C. Louis and D.H. White, Phys. Rev. **C48** (1993) 761.

- [61] B.A. Campbell, J. Ellis and R.A. Flores, Phys. Lett. **B225** (1989) 419.
- [62] D. Bruss, T. Gasenzer and O. Nachtmann, Phys. Lett. **A239** (1998) 81; hep-ph/9802317.
- [63] G. Altarelli and B. Lampe, Z. Phys. **C47** (1990) 315;
G. Altarelli, Proc. Physics at HERA, Vol. 1 (1991) 379, eds. W. Buchmüller and G. Ingelman.
- [64] G.C. Fox and D.Z. Freedman, Phys. Rev. **182** (1969) 1628;
D. Broadhurst, J. Gunion and R.L. Jaffe, Phys. Rev. **D8** (1973) 566; Ann. Phys. **81** (1973) 88.
- [65] S.L. Adler and R.F. Dashen, *Current Algebras and Applications to Particle Physics* (W.A. Benjamin, 1968).
- [66] H. Fritzsch and P. Minkowski, Nuovo Cim. **30A** (1975) 393.
- [67] G. Christos, Phys. Rept. **116** (1984) 251.
- [68] E. Witten, Nucl. Phys. **B156** (1979) 269;
G. Veneziano, Nucl. Phys. **B159** (1979) 213.
- [69] G. 't Hooft, Phys. Rev. Lett. **37** (1976) 8; Phys. Rev. **D14** (1976) 3432.
- [70] G. 't Hooft, Phys. Rept. **142** (1986) 357.
- [71] P. Minkowski, Phys. Lett. **B237** (1990) 531; **B423** (1998) 157.
- [72] S.J. Brodsky, J. Ellis and M. Karliner, Phys. Lett. **B206** (1988) 309.
- [73] G.M. Shore and G. Veneziano, Nucl. Phys. **B516** (1998) 333.
- [74] D. de Florian, G.M. Shore and G. Veneziano, hep-ph/9711353, *in* Proc. Workshop on *Physics with Polarized Protons at HERA*, eds. A. De Roeck and T. Gehrmann, DESY-Proceedings-1998-01
- [75] A. De Roeck and T. Gehrmann, hep-ph/9711512, *in* Proc. Workshop on *Physics with Polarized Protons at HERA*, eds. A. De Roeck and T. Gehrmann, DESY-Proceedings-1998-01
- [76] The PHOENICS Collaboration (A. Bock et al), Phys. Rev. Lett. **81** (1998) 534.
- [77] The TAPS Collaboration (B. Krusche et al.), Phys. Rev. Lett. **74** (1995) 3736.
- [78] CEBAF experiments E-89-039 (S. Dytman et al.) and E-91-008 (B.G. Ritchie et al.).

- [79] S. Tapprogge, Talk at the Workshop *Pomeron and Odderon in Theory and Experiment* (Heidelberg, March 1998);
<http://www.tphys.uni-heidelberg.de/ws/>
- [80] CELSIUS (H. Calen et al.), Phys. Rev. Lett. **80** (1998) 2069;
The WASA Collaboration (R. Bilger et al.), Nucl. Phys. **A626** (1997) 93c.
- [81] The COSY-11 Collaboration (P. Moskal et al.), Phys. Rev. Lett. **80** (1998) 3202.
- [82] The WA102 Collaboration (D. Barberis et al.), Phys. Lett. **B427** (1998) 398.
- [83] The CLEO Collaboration (J. Gronberg et al.), Phys. Rev. **D57** (1998) 33.
- [84] The CLEO Collaboration (B.H. Behrens et al.), Phys. Rev. Lett. **80** (1998) 3710;
The CLEO Collaboration (T.E. Browder et al.), Phys. Rev. Lett. **81** (1998) 1786;
J.G. Smith, hep-ex/9803028.
- [85] H. Fritzsche, Phys. Lett. **B415** (1997) 83.
- [86] R.L. Jaffe, Phys. Lett. **B365** (1996) 359.
- [87] A.V. Manohar, Phys. Rev. Lett. **65** (1990) 2511.
- [88] J. Kogut and L. Susskind, Phys. Rev. **D11** (1974) 3594.
- [89] C. Cronström and J. Mickelsson, J. Math. Phys. **24** (1983) 2528.
- [90] S.L. Adler, in Brandeis *Lectures on Elementary Particles and Quantum Field Theory*, eds. S. Deser, M. Grisaru and H. Pendleton (MIT Press, 1970).
- [91] R.J. Crewther, Riv. Nuovo Cimento **2** (1979) 63, section 7.
- [92] J. Bardeen, L. Cooper and J. Schrieffer, Phys. Rev. **108** (1957) 1175.
- [93] P.W. Anderson and W.F. Brinkman, Theory of Anisotropic Superfluidity in He^3 , in *The Helium Liquids: Proc. 15th Scottish Universities Summer School in Physics 1974*, eds. J.G.M. Armitage and I.E. Farquhar (Academic Press, New York, 1975).
- [94] S. Grebenev, J.P. Toennies and A.F. Vilesov, Science **279** (1998) 2083.
- [95] M.A. Shifman, A.I. Vainshtein and V.I. Zakharov, Nucl. Phys. **B147** (1979) 385, 448;
E.V. Shuryak, Phys. Rept. **115** (1984) 151.

- [96] S.D. Bass, B.L. Ioffe, N.N. Nikolaev and A.W. Thomas, J. Moscow Phys. Soc. **1** (1991) 317.
- [97] L. Mankiewicz and A. Schäfer, Phys. Lett. **B242** (1990) 455;
L. Mankiewicz, Phys. Rev. **D43** (1991) 64.
- [98] G.T. Bodwin and J. Qiu, Phys. Rev. **D41** (1990) 2755.
- [99] A.V. Manohar, Phys. Rev. Lett. **66** (1991) 289.
- [100] P. Ratcliffe, Nucl. Phys. **B223** (1983) 45.
- [101] S.D. Bass, N.N. Nikolaev and A.W. Thomas, Adelaide University preprint ADP-133-T80 (1990) unpublished;
S.D. Bass, Ph.D. thesis (University of Adelaide, 1992).
- [102] S.D. Bass, Z Physik **C55** (1992) 653.
- [103] H.-Y. Cheng, Phys. Lett. **B427** (1998) 371.
- [104] M. Stratmann, hep-ph/9710379 in Proc. Workshop on *Deep Inelastic Scattering off Polarized Targets: Theory meets Experiment*, DESY-Zeuthen 1997, eds. J. Blümlein et al. (DESY report 97-200, 1997).
- [105] M. Gluck, E. Reya, M. Stratmann and W. Vogelsang, Phys. Rev. **D53** (1996) 4775.
- [106] J. Ellis, M. Karliner and C.T. Sachrajda, Phys. Lett. **B231** (1989) 497.
- [107] G.P. Lepage and S.J. Brodsky, Phys. Rev. **D22** (1980) 2157.
- [108] S.D. Bass, S.J. Brodsky and I. Schmidt, Phys. Lett. **B437** (1998) 417.
- [109] G. Altarelli and G. Parisi, Nucl. Phys. **B126** (1977) 298.
- [110] R. Mertig and W.L. van Neervan, Z Phys. **C70** (1996) 637;
E.B. Zijlstra and W.L. van Neervan, Nucl. Phys. **B417** (1994) 61; (E) **B426** (1994) 245.
- [111] W. Vogelsang, Phys. Rev. **D54** (1996) 2023.
- [112] E. Leader, A.V. Sidorov and D.B. Stamenov, Phys. Lett. **B445** (1998) 232.
- [113] T. Gehrmann and W.J. Stirling, Phys. Rev. **D53** (1996) 6100.
- [114] G. Altarelli, R.D. Ball, S. Forte and G. Ridolfi, Nucl. Phys. **B496** (1997) 337.
- [115] D. de Florian, O.A. Samapayo and R. Sassot, Phys. Rev **D57** (1998) 5803.

- [116] L.E. Gordon, M. Goshtasbpour and G.P. Ramsey, Phys. Rev. **D58** (1998) 094017.
- [117] The E-154 Collaboration (K. Abe et al.), Phys. Lett. **B405** (1997) 180.
- [118] G. 't Hooft and M. Veltman, Nucl. Phys. **B44** (1972) 189.
- [119] R.D. Ball, S. Forte and G. Ridolfi, Phys. Lett. **B378** (1996) 255.
- [120] C.H. Llewellyn Smith, hep-ph/9812301.
- [121] The COMPASS proposal, CERN/SPSLC 96-14.
- [122] The HERMES Charm Upgrade Program, HERMES 97-004.
- [123] P. Bosted, private communication.
- [124] N. Hayashi, Y. Goto and N. Saito, hep-ex/9807033.
- [125] Proc. Workshop on *Physics with Polarized Protons at HERA*, eds. A. De Roeck and T. Gehrmann, DESY-Proceedings-1998-01
- [126] L.L. Frankfurt et al., Phys Lett. **B230** (1989) 141.
- [127] F.E. Close and R.G. Milner, Phys. Rev. **D44** (1991) 3691.
- [128] The SMC Collaboration (B. Adeva et al), Phys. Lett. **B420** (1998) 180.
- [129] W. Wislicki, Mod. Phys. Lett. **A13** (1988) 405.
- [130] J. Kuti and V. Weisskopf, Phys. Rev. **D4** (1971) 3418.
- [131] F.E. Close, Nucl. Phys. **B80** (1974) 269.
- [132] R. Carlitz and J. Kaur, Phys. Rev. Lett. **38** (1977) 673.
- [133] H. Weigel, L. Gamberg and H. Reinhardt, Phys. Rev. **D55** (1997) 6910;
O. Schroder, H. Reinhardt and H. Weigel, Phys. Lett. **B439** (1998) 398.
- [134] S.J. Brodsky, M. Burkardt and I. Schmidt, Nucl. Phys. **B441** (1995) 197.
- [135] C. Young in Proc. Workshop on *Deep Inelastic Scattering off Polarized Targets: Theory meets Experiment*, DESY-Zeuthen 1997, eds. J. Blümlein et al. (DESY report 97-200, 1997).
- [136] J. Soffer and O.V. Teryaev, Phys.Rev. **D56** (1997) 1549.
- [137] S.D. Bass and M.M. Brisudová, hep-ph/9711423, Euro. Phys. J **A** (in press).

- [138] R.L. Heimann, Nucl. Phys. **B64** (1973) 429.
- [139] J. Ellis and M. Karliner, Phys. Lett. **B213** (1988) 73.
- [140] P.V. Landshoff, Proc. Zuoos Summer School, PSI Proceedings 94-01 (1994) 135, hep-ph/9410250.
- [141] The New Muon Collaboration (M. Arneodo et al.), Nucl. Phys. **B483** (1997) 3.
- [142] B. Badelek and J. Kwieciński, Phys. Lett. **B418** (1998) 229.
- [143] Various contributions in Proc. Workshop on *Deep Inelastic Scattering off Polarized Targets: Theory meets Experiment*, DESY-Zeuthen 1997, eds. J. Blümlein et al. (DESY report 97-200, 1997).
- [144] L. Galfi, J. Kuti and A. Patkos, Phys. Lett. **B31** (1970) 465;
J. Kuti, Erice lectures (1995), in Proc. Erice School *The spin structure of the nucleon*, eds. B. Frois and V. Hughes (World Scientific, 1997).
- [145] F.E. Close and R.G. Roberts, Phys. Rev. Lett. **60** (1988) 1471; Phys. Lett. **B336** (1994) 257.
- [146] S.D. Bass and P.V. Landshoff, Phys. Lett. **B336** (1994) 537.
- [147] R. Kirschner and L.N. Lipatov, Nucl. Phys. **B213** (1983) 122.
- [148] J. Bartels, B.I. Ermolaev and M.G. Ryskin, Z Phys **C70** (1996) 273; **C72** (1996) 627.
- [149] J. Blümlein and A. Vogt, Phys. Lett. **B386** (1996) 350.
- [150] K. Gottfried, Phys. Rev. Lett. **18** (1967) 1174.
- [151] The New Muon Collaboration (M. Arneodo et al.), Phys. Rev. **D50** (1994) R1.
- [152] The E866/NuSea Collaboration (E.A. Hawker et al.), Phys. Rev. Lett. **80** (1998) 3715.
- [153] A.W. Thomas, Phys. Lett. **B126** (1983) 97.
- [154] R.D. Field and R.P. Feynman, Phys. Rev. **D15** (1977) 2590.
- [155] A. W. Thomas and W. Melnitchouk, in *New Frontiers in Nuclear Physics*, eds. S. Homma, Y. Akaishi and M. Wada (World Scientific, Singapore, 1993), pp. 41-106.

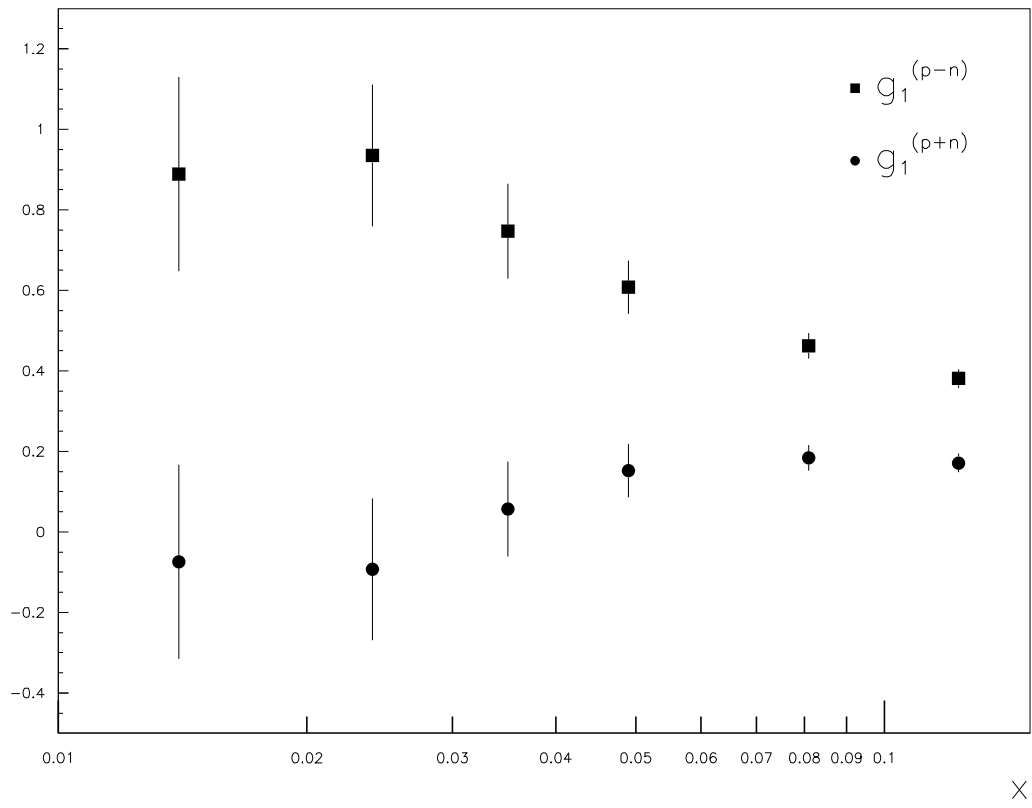


Figure 1: The SLAC data on $g_1^{(p-n)}$ at small x . The proton data is taken from E-143 [8] and E-155 [135] (two smallest x data points). The neutron data is taken from E-154 [9].

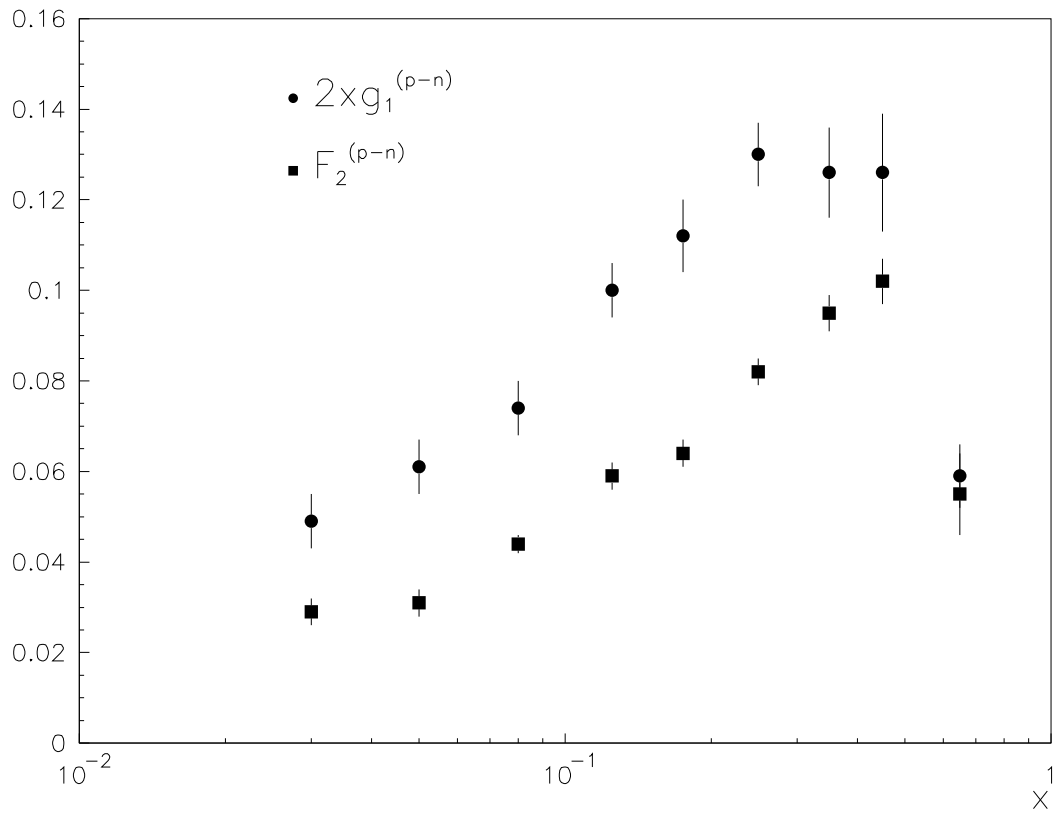


Figure 2: The isotriplet structure functions $2xg_1^{(p-n)}$ and $F_2^{(p-n)}$. The $g_1^{(p-n)}$ data is from SLAC, the $F_2^{(p-n)}$ data is from NMC.

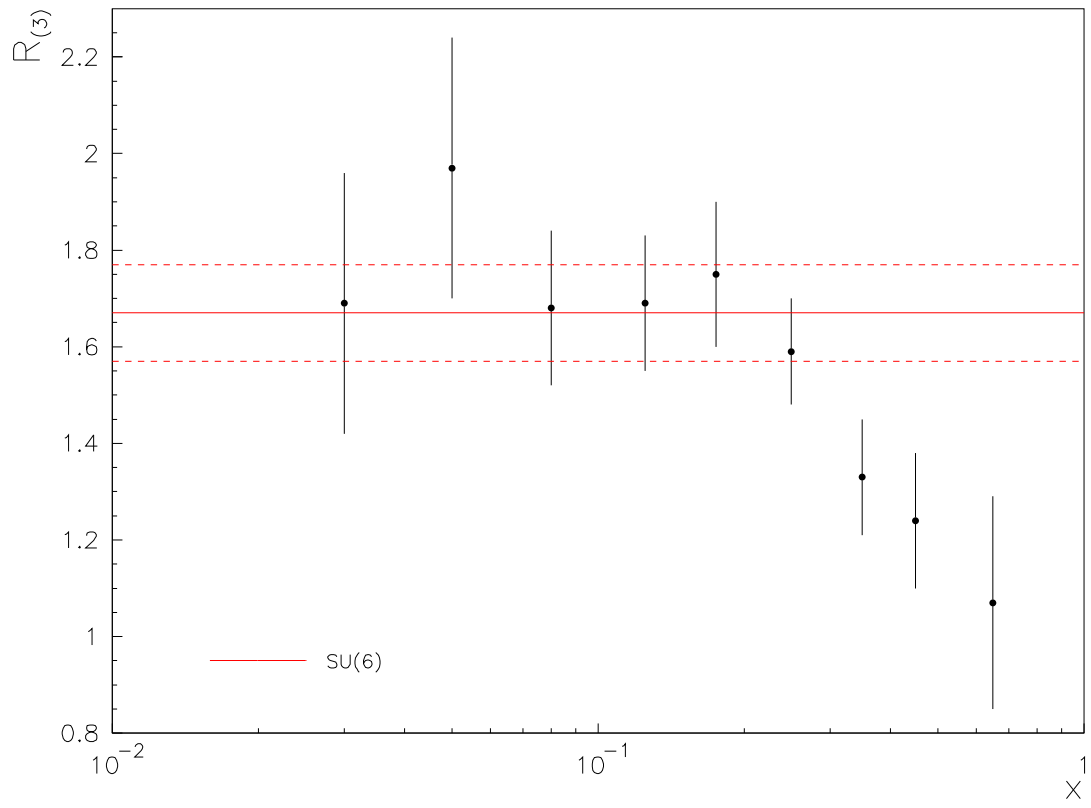


Figure 3: The ratio $R_{(3)} = 2xg_1^{(p-n)}/F_2^{(p-n)}$ obtained from the $g_1^{(p-n)}$ and $F_2^{(p-n)}$ data in Fig.2.